Treatment of Non-small cell lung cancer with AiDi injection based on network pharmacology

Suishan Qiu
The First Affiliated Hospital of Jinan University
Lianfang Xue
The First Affiliated Hospital of Jinan University
Hui Liu (liu_ui@hotmail.com)
The First Affiliated Hospital of Jinan University https://orcid.org/0000-0001-7422-6297
Huiting Zhong
The First Affiliated Hospital of Jinan University
Leping Li
The First Affiliated Hospital of Jinan University

Research

Keywords: Medicine, Chinese Traditional, Pharmacologic Actions, Carcinoma, Non-Small-Cell Lung

Posted Date: November 13th, 2020

DOI: https://doi.org/10.21203/rs.3.rs-104145/v1

Abstract

Background: This study aimed to determine the bioactive compounds, core genes, and pharmacological mechanisms underlying the effects of Aidi injection (ADI) in non-small cell lung cancer (NSCLC), and to provide a further research directions.

Material and Methods: The bioactive compounds of ADI were obtained from the Traditional Chinese Medicine Systems Pharmacology Database and the Traditional Chinese Medicines Integrated Database, while targets related to these bioactive compounds and NSCLC were obtained from the GEO database. Cytoscape software was used to construct ingredients–protein-targets–pathway networks. Gene Ontology and Kyoto Encyclopedia of Genes and Genomes pathway analyses and network analysis were performed to investigate potential mechanisms underlying the effects of ADI on NSCLC.

Results: This study screened 45 bioactive compounds and 38 major proteins of ADI as potential agents that can act against NSCLC. The results revealed the following potential therapeutic targets of ADI in the treatment of NSCLC: FOS, VEGFA, EGFR, JUN, MMP9, IL2, STAT1, CASP1, NFKBA, and CDK2. The potential mechanisms via which ADI acts against NSCLC are closely related to the inhibition of apoptosis and the activation of signaling pathways.

Conclusion: This study has revealed the multicompound, multitarget, and multichannel characteristics of ADI. This provides novel insight into further research investigations of the mechanism of ADI in NSCLC treatment.

Background

Lung cancer is the human cancer with the highest mortality rate among all cancers worldwide, and is frequently diagnosed as one of the most malignant [1, 2]. Non-small cell lung cancer (NSCLC) is the most-frequent histological subtype of lung cancer. Despite many effective therapeutic approaches being applied, including surgery, chemotherapy, radiotherapy, targeted therapy, and immunotherapy, the 5-year survival rate of lung cancer remains too low [3].

An Aidi injection (ADI) involves the herbs cantharides, ginseng, astragalus, and acanthopanax, and is mainly used to treat primary liver cancer, lung cancer, rectal cancer, malignant lymphomas, and gynecological malignant tumors. Cantharidin is the active component of cantharides, and it can slow down the synthesis of RNA and DNA as well as progression of the cell cycle by inhibiting the synthesis of proteins in tumor cells, which will increase the apoptosis of tumor cells and inhibit their proliferation [4]. A canthopanax improves the tolerance and adaptability of the body and regulates its immune function [5]. The antitumor mechanism of astragalus includes regulating immune function, promoting the apoptosis of tumor cells, inhibiting tumor angiogenesis, and affecting amino-acid metabolism [6, 7]. The anti-metastasis effect of ginsenoside Rg3 is related to its inhibition of the invasion, adhesion, and anti-angiogenesis of tumor cells [8]. However, the active components and molecular mechanism underlying its action in the treatment of NSCLC remain to be fully clarified.

Traditional Chinese medicine (TCM) is based on multiple targets, multiple pathways, and multiple components. Network pharmacology refers to the theory of system biology that emphasizes the multichannel regulation of certain pathways. Constructing a network of components to analyze their relationship while focusing on the key nodes in the network allows the material basis and mechanism of action of TCM and its associated drug compounds to be systematically elaborated. This approach is currently mainly used in research into the mechanisms of action of TCM and the associated compound drugs and the development of new drugs [9]. In addition, many studies have been conducted on TCM preparations and cancer mechanisms based on network pharmacology [10].

Based on the aforementioned background, this study used network pharmacology to predict the molecular biological mechanisms underlying the efficacy of ADI in NSCLC. The aim was to provide a methodological and theoretical basis for diagnosis and treatment when integrating TCM, Western medicine, and basic experimental research. Figure 1 shows the work flowchart of this study.

Material And Methods

Components of ADI

We searched the Traditional Chinese Medicine Systems Pharmacology Database (TCMSP; http://lsp.nwu.edu.cn/) and the Traditional Chinese Medicines Integrated Database(TCMID; https://omictools.com/tcmid-tool) to determine the chemical ingredients of the four herbs contained in an ADI. The TCMSP database was searched using “cantharides”, “astragalus”, and “ginseng” as keywords to retrieve the active components of each drug used in TCM using screening conditions of an oral bioavailability (OB) of ≥ 30% and a drug likeness (DL) of ≥ 0.18%. When using “acanthopanax” as the keyword, the active components were searched in the TCMID and TCMSP for which OB ≥ 30% and DL ≥ 0.18.

Predicting the known therapeutic targets acting on NSCLC

We collected NSCLC targets from the GEO database (https://www.ncbi.nlm.nih.gov/geo/), which is a gene-expression database created and maintained by the NCBI (National Center for Biotechnology Information) in the United States. This database includes high-throughput gene-expression data submitted by research institutions world wide. The GEO database was searched using “NSCLC” as the keyword, “Homo sapiens” as the species, and “Series” as then try type to identify the relevant chip. The R software was used to analyze the original data of the chip. The robust-multiarray-average algorithm was used for background correction and to normalize the matrix data. The limma package was used to analyze the different genes in the chip data. The screening conditions for identifying significantly different genes were set as a P value of < 0.05 and a relative change of > 1.2×. The R plot package was used to draw the original volcano diagram of the chip.

Intersection target

The common targets for drugs and diseases are obtained using the Venny (version 2.1.0; https://bioinfogp.cnb.csic.es/tools/venny/) online tools, The common targets can be considered as the targets of ADI in the treatment of NSCLC.

Disease–compound–target network construction

The selected intersecting targets and the active components and their corresponding potential targets were imported into the Cytoscape software to generate a network diagram of the interaction between active components and targets. A topological analysis was then performed.

Construction of the protein–protein interaction network

The STRING database (https://string-db.org/) can be used to analyze protein–protein interactions (PPI). In our study the species was limited to *Homo sapiens*, the lowest interaction score was set to medium confidence (= 0.40), discrete targets were hidden, and the remaining parameters were kept at their default settings. The PPI network identified in the STRING database was visualized and then further analyzed using Cytoscape software.

Enrichment analysis of the GO and KEGG pathways

The Metascape platform (http://metascape.org/) provides powerful functions that allow the integration of several authoritative databases, such as Gene Ontology (GO), Kyoto Encyclopedia of Genes and Genomes (KEGG), and Uniprot, and it can be used for the pathway enrichment analysis of gene targets. It is updated monthly to ensure the accuracy of the data. This platform was used to analyze the GO and KEGG for the candidate targets. The GO database includes three parts for interpreting the antitumor biological processes involved with key targets: molecular function (MF), biological process (BP), and cellular component (CC). Enrichment analysis was applied to the KEGG data in order to investigate the main antitumor signaling pathways involved in key targets. Based on the relevant targets identified from the KEGG results, a path–target–compound network was constructed to further screen the key target genes and active components involved when treating NSCLC using ADI.

Results

Composite ingredients of ADI

Under the conditions of OB ≥ 30% and DL ≥ 0.18%, astragalus and ginseng were obtained by searching the TCMSP, while acanthopanax was obtained by searching the TCMID. This analysis identified 45 active components of ADI.

NSCLC GEO chip heat and volcano maps

The GSE21933 chip and platform data were downloaded from the GEO database with 42 samples, and R software was used to draw heat maps (Fig. 1) and volcano maps (Fig. 2). In the maps, the color

saturation indicates the degree of gene expression, with redder and greener colors indicating more- and less-significant gene expression, respectively.

Intersection target

The application of the Venny online tools revealed 61 common targets for drugs and diseases, as shown in Fig. 3.

Disease–compound–target network and analysis

A disease–compound–target network was constructed based on the 45 bioactive compounds and their targets. Figure 4 shows that quercetin (MOL000098), kaempferol (MOL000422), sitosterol (MOL000358), isorhamnetin (MOL000354), and 7-0-methylisoeugenol (MOL000378) were the most-important components of the ADI. These findings show that ADI treats NSCLC through the combined action of multiple components and targets.

Analysis of the PPI network

The PPI network diagram was constructed by importing the intersection target into the STRING database, exporting the data in TSV file format, and importing the data into Cytoscape software. Figure 5 shows the produced network, which included 61 nodes and 214 edges. The network-analyzer plug-in in Cytoscape software was used to analyze the topological parameters of the network graph, with the following top-10 core targets identified using a degree criterion of ≥ 7 (Fig. 6):FOS, VEGFA, EGFR, JUN, MMP9, IL2, STAT1, CASP1, NFKBA, and CDK2.

Enrichment analysis of the GO and KEGG pathways

Intersection targets were imported into the Metascape platform. The BPof ADI in the treatment of NSCLC includes the response to organic substances, the response to mechanical stimulus, the cellular responses to oxygen-containing compounds, coenzyme metabolic process, the response to reactive oxygen species, and the cellular responses to reactive oxygen species, as shown in Fig. 7. The CC includes enuclear chromatin and the mitochondrial matrix, transcription factor complex, membrane raft, membrane microdomain, and membrane region (Fig. 8), while the MF includes coenzyme binding, vitamin binding, lyase activity, carboxylic acid binding, organic acid binding, DNA-binding transcription activator activity, and RNA polymerase II specificity (Fig. 9).

Figure 10 shows the results obtained by analyzing components of the KEGG pathway that participate in the treatment of NSCLC by ADI, including bladder cancer, hepatitis B, the relaxin signaling pathway, human T-cell leukemia virus 1 infection, prostate cancer, the C-type lectin receptor signaling pathway, interleukin (IL)-17-producing helper T (Th17) cell differentiation, and the tumor necrosis factor (TNF) signaling pathway.

Discussion

TCM utilizes a multicomponent and multitarget synergistic system that accounts for the complexity of various herbal components acting on multiple targets and diseases. These ingredients with distinct effects and targets can act on various aspects of a disease via multiple systems, and they interact to produce synergistic effects [11, 12]. Network pharmacology can be used to predict the target profiles and pharmacological actions of herbal compounds. The present study used network-construction approaches to identify the bioactive compounds in ADI and their potential targets, and to determine the mechanisms underlying the effects of ADI in NSCLC.

Our topological analysis of the component drugs and target interaction network revealed that the active ingredients that may play important roles in ADI are quercetin, kaempferol, sitosterol, isorhamnetin, 7-O-methylisomucronulatol, formononetin, and cantharidin. Quercetin is a flavonoid compound that functions as an antioxidant, scavenging free radicals and lowering blood lipid and blood glucose levels [13, 14]. Quercetin inhibits the activity of NSCLC cells by regulating the mir-16/HOXA10 axis, and promotes the apoptosis of NSCLC cancer cells [15]. Quercetin may inhibit the STAT3 signaling pathway, inhibit the migration and invasion of A549 cells, and induce the apoptosis of tumor cells [16].

Kaempferol exerts numerous pharmacological effects, including anti-oxidation, ant-ivirus, anti-bacterial, and anti-cancer effects. By inhibiting ERR beam, kaempferol reduces the invasion and migration of NSCLC A549 cells [17],inhibits the proliferation of H446 cells in small-cell lung cancer, inhibits H446 cells in the S and G2/M phases of the cell cycle, and induces the apoptosis of H446 cells [18].

Cantharidin is the effective medicinal component of cantharides that exerts beneficial effects against malignant tumors such as liver cancer, esophageal cancer, lung cancer, and gastric cancer [19]. Cantharidin inhibits the activity of caspase-3 and caspase-7 downstream of the apoptotic pathway via the expression of survivin, thereby inducing apoptosis [20].

Formononetin can induce the apoptosis of human colon and prostate cancer cells. The mechanism via which formononetin inhibits the proliferation of lung cancer A549 cells may be related to the induction of apoptosis and down-regulation of the expression level of bcl-2 [21].

Isorhamnetin and quercetin are both flavonoid compounds. Recent studies have found that isorhamnetin exhibits beneficial cardiovascular effects such as anti-myocardial hypoxia and ischemia, relieving angina pectoris, anti-arrhythmia effects, inhibiting antioxidant free radicals, and lowering serum cholesterol [22]. The anti-cancer effect of isorhamnetin is associated with the induction of apoptosis, which may change the expression of apoptosis-related genes such as down-regulating the expression of bcl-2 and changing the bcl-2/Bax ratio by regulating members of the bcl-2 protein family [23]. Isorhamnetin down-regulates the expression of bcl-2 gene and PCNA protein. Isorhamnetin also up-regulates the tumor suppressor genes P53, Bax, and caspase-3, and so it may mainly act by inhibiting the DNA synthesis of tumor cells. The up-regulation or down-regulation of apoptosis-related genes induces the apoptosis of cancer cells to inhibits their proliferation and growth [24].

VEGFA binds to its receptor-2 (VEGFAR-2) to promote the proliferation, growth, and survival of vascular endothelial cells. The expression of VEGFA is increased in malignant tumor cells, which is associated with the level of VEGFAR-2 being up-regulated to enhance tumor growth and proliferation [25]. Wei et al. found that VEGFA promoted the growth and proliferation of NSCLC tumor cells and accelerated tumor progression [26]. C-JUN is a major member of the AP-1 family of nuclear transcription factors. Phosphorylation and activation by P-JNK results in C-JUN forming homologous or heterodimers with transcription factors such as C-FOS, activating and initiating the expression of downstream target gene cyclin D1, regulating the cell cycle, and promoting cell proliferation [27].

Tumor metastasis is a complex process involving intracellular signal transduction. Tumor cells synthesize and secrete MMP to degrade the extracellular matrix and promote their own invasion and metastasis [28]. MMP9 is an important member of the family of MMPs that is closely related to tumor invasion and metastasis, and its expression is up-regulated in various tumor tissues [29]. FOXC2 may promote the invasion and migration of NSCLC cells by up-regulating MMP9[30]. CASP1 regulates tumors in two ways [31]: (1) by mediating the release of IL-1β, which plays a key regulatory role in the occurrence and development of tumors by regulating the development of myeloid cells in peripheral tissues and tumor microenvironment [32], and (2)by inhibiting tumor growth by activating the acquired immunity or apoptosis of tumor cells.CASP1 exists in cells without an active enzyme progenitor, and is activated by the macromolecule ASC dimer [32], which further catalyzes the proteolysis of caspase-7 and other acting substrates, leading to apoptosis [34].

The results obtained in the analysis of KEGG-pathway enrichment were mainly related to cancer pathways, hepatitis B, the relaxin signaling pathway, the TNF signaling pathway, the C-type lectin receptor signaling pathway, Th17 cell differentiation, the IL-17 signaling pathway, and human T-cell leukemia virus 1 infection. The IL-17 family includes a subset of cytokines consisting of IL-17A to IL-17AF, which play crucial roles in both acute and chronic inflammatory responses. The IL-17-family protein signal via their correspondent receptors to activate downstream pathways that include NF-kappa, MAPKs, and C/EBPs to induce the expression of antimicrobial peptides, cytokines, and chemokines. Human T-cell leukemia virus type 1 is a pathogenic retrovirus that is associated with adult T-cell leukemia/lymphoma. The pathogenesis is critically affected by the expression of the viral regulatory protein Tax, which is a transcriptional cofactor that interferes in several signaling pathways related to anti-apoptosis and cell proliferation.

TNF is a critical cytokine that can induce a wide range of intracellular signal pathways, including those related to apoptosis, cell survival, inflammation, and immunity. Th17 cells serve as a subset of $CD4^+$ T cells involved in immune responses mediated by epithelial cells and neutrophils against extracellular microbes, and they are involved in the pathogenesis of autoimmune diseases. We found that these signaling pathways are closely related to NSCLC, and the active components in ADI can exert treatment effects against that cancer via these signaling pathways.

This study utilized network pharmacology to analyze the mechanisms underlying the effects of ADI in treating NSCLC. This approach has yielded important information for improving the understanding of compound–target–disease interactions, and also for providing ideas and acting as the basis for further studies. However, this study was subject to some limitations. The mechanism of action of ADI was only analyzed theoretically, and the predicted results might not be correct. Also, network information technology is not yet fully developed, and the analyzed databases are not completely up to date.

Notwithstanding the above limitations, this study applied bioinformatics and network pharmacology to explore the multicomponent and multitarget characteristics of ADI in treating cancer. We have identified that ADI involves 33 active ingredients that act against NSCLC, and some of their active anticancer effects have been confirmed in previous studies, such as for quercetin, kaempferol, sitosterol, isorhamnetin, 7-O-methylisomucronulatol, formononetin, and cantharidin. Our enrichment analysis revealed that the TNF signaling pathway, the C-type lectin receptor signaling pathway, Th17-cell differentiation, the IL-17 signaling pathway, and human T-cell leukemia virus 1 infection are important anti-NSCLC mechanisms of the active components in ADI.

Conclusion

The comprehensive data obtained in this study can provide a theoretical basis for screening candidate anticancer drugs. Future studies should attempt to perform in vitro and in vivo experimental verifications of the active ingredients in ADI.

Abbreviations

ADI: Aidi injection; NSCLC: non-small cell lung cancer; TCM: Traditional Chinese medicine; TCMSP: Traditional Chinese Medicine Systems Pharmacology Database;

TCMID: Traditional Chinese Medicines Integrated Database; OB: oral bioavailability; DL: drug likeness; PPI: protein–protein interactions; GO: Gene Ontology; KEGG: Genes and Genomes; MF: molecular function; BP: biological process; CC: cellular component; Th17: interleukin (IL)-17-producing helper T; TNF: tumor necrosis factor; VEGFAR-2: VEGFA binds to its receptor-2.

Declarations

Acknowledgements

No applicable.

Authors' contributions

SQ and LX designed the study, HL and HZ analyzed the data; LL wrote the article. All authors read and approved the final manuscript.

Funding

This work was financially supported by the research project of Guangdong Provincial Bureau of traditional Chinese Medicine (No. 20191089 and No. 20201082) and Guangdong Provincial Hospital Pharmaceutical Research Fund (No. 2020A27).

Availability of data and materials

All data of the databases are available.

Ethics approval and consent to participate

Ethics approval not applicable. The data do not compromise anonymity or confidentiality or breach local data protection law.

Consent for publication

Not applicable.

Competing interests

The authors declare to have no competing interests.

Author details

[1] Department of Pharmacy, The First Affiliated Hospital of Jinan University, Guangzhou 510630, China

References

1. Poston G J. Global cancer surgery: The Lancet Oncology review. European Journal of Surgical Oncology. 2015;41:1559-61.
2. Bray F, Ferlay J, Soerjomataram I, et al. Global cancer statistics 2018: GLOBOCAN estimates of incidence and mortality worldwide for 36 cancers in 185 countries. CA Cancer J Clin. 2018;68:394-424.
3. Ettinger D S. Ten years of progress in non-small cell lung cancer. Journal of the National Comprehensive Cancer Network. 2012;10:292.
4. Yan M S, Xiue S, Wei L X, et al. The preliminary observation on immunosuppressive effect of norcantharidin in mice. Immunopharmacol Immunotoxicol. 1993;15:79-85.
5. Wang G S. Medical uses of mylabris in ancient China and recent studies. J Ethnopharmacol. 1989;26:147-62.
6. Guo L, Hua J, Luan Z, et al. Effects of the stems and leaves of Astragalus membranaceus on growth performance, immunological parameters, antioxidant status, and intestinal bacteria of quail. Anim Sci J. 2019;90:747-56.

7. Wang E, Liu T, Lu X, et al. Comparison of aerial parts of Astragalus membranaceus and Astragali Radix based on chemical constituents and pharmacological effects. Food and Agricultural Immunology. 2019;30:1046-66.
8. Mochizuki M, Yoo Y C, Matsuzawa K, et al. Inhibitory effect of tumor metastasis in mice by saponins, ginsenoside-Rb2, 20(R)- and 20(S)-ginsenoside-Rg3, of red ginseng. Biol Pharm Bull. 1995;18:1197-202.
9. Liu H, Zeng L, Yang K, et al. A Network Pharmacology Approach to Explore the Pharmacological Mechanism of Xiaoyao Powder on Anovulatory Infertility. Evid Based Complement Alternat Med. 2016;2016:2960372.
10. Hopkins A L. Network pharmacology: the next paradigm in drug discovery. Nature Chemical Biology. 2008;4:682-90.
11. Li B, Xu X, Wang X, et al. A systems biology approach to understanding the mechanisms of action of chinese herbs for treatment of cardiovascular disease. International journal of molecular sciences. 2012;13:13501-20.
12. Zhao F, Guochun L, Yang Y, et al. A network pharmacology approach to determine active ingredients and rationality of herb combinations of Modified-Simiaowan for treatment of gout. J Ethnopharmacol. 2015;168:1-16.
13. Boots A W, Haenen G R, Bast A. Health effects of quercetin: from antioxidant to nutraceutical. Eur J Pharmacol. 2008;585:325-37.
14. Baby B, Antony P, Vijayan R. Interactions of quercetin with receptor tyrosine kinases associated with human lung carcinoma. Natural Product Research. 2017;32:2928-31.
15. Wang Q, Chen Y, Lu H, et al. Quercetin radiosensitizes non-small cell lung cancer cells through the regulation of miR-16-5p/WEE1 axis. IUBMB Life. 2020;72:1012-22.
16. Harada D, Takigawa N, Kiura K. The Role of STAT3 in Non-Small Cell Lung Cancer. Cancers. 2014;6:708-22.
17. Nguyen T T, Tran E, Ong C K, et al. Kaempferol-induced growth inhibition and apoptosis in A549 lung cancer cells is mediated by activation of MEK-MAPK. J Cell Physiol. 2003;197:110-21.
18. Vaseva A V, Moll U M. The mitochondrial p53 pathway. Biochim Biophys Acta. 2009;1787:414-20.
19. Li H, Xia Z, Chen Y, et al. Cantharidin Inhibits the Growth of Triple-Negative Breast Cancer Cells by Suppressing Autophagy and Inducing Apoptosis in Vitro and in Vivo. Cellular Physiology and Biochemistry. 2018;43:1829-40.
20. Zhang W, Zhao H, Yan Y, et al. Apoptosis of human lung cancer A549 cells induced by cantharidin and its molecular mechanism. Chinese journal of cancer. 2005:330-4.
21. Yang Y, Zhao Y, Ai X, et al. Formononetin suppresses the proliferation of human non-small cell lung cancer through induction of cell cycle arrest and apoptosis. International journal of clinical and experimental pathology. 2014;7:8453.

22. Wang Z R, Wang L, Yin H H, et al. Effect of total flavonoids of hippophae rhamnoides on contractile mechanics and calcium transfer in stretched myocyte. Space Med Med Eng (Beijing). 2000;13:6-9.
23. Li Q, Ren F Q, Yang C L, et al. Anti-proliferation effects of isorhamnetin on lung cancer cells in vitro and in vivo. Asian Pac J Cancer Prev. 2015;16:3035-42.
24. Radhakrishna Pillai G, Srivastava A S, Hassanein T I, et al. Induction of apoptosis in human lung cancer cells by curcumin. Cancer Letters. 2004;208:163-70.
25. Roskoski R J. Vascular endothelial growth factor (VEGF) signaling in tumor progression. Crit Rev Oncol Hematol. 2007;62:179-213.
26. Wei C, Zhang J, Li B, et al. Advances in the study of anti-tumor natural compounds targeting VEGF/VEGFR. Chinese herbal medicine. 2017;48:5049-56.
27. Vairaktaris E, Loukeri S, Vassiliou S, et al. EGFR and c-Jun exhibit the same pattern of expression and increase gradually during the progress of oral oncogenesis. In Vivo. 2007;21:791-6.
28. Talvensaari-Mattila A, Pääkkö P, Turpeenniemi-Hujanen T. Matrix metalloproteinase-2 (MMP-2) is associated with survival in breast carcinoma. British Journal of Cancer. 2003;89:1270-5.
29. Darlix A, Lamy P J, Lopez-Crapez E, et al. Serum NSE, MMP-9 and HER2 extracellular domain are associated with brain metastases in metastatic breast cancer patients: predictive biomarkers for brain metastases? Int J Cancer. 2016;139:2299-311.
30. Hu Y, Zhu J. Expression and clinical significance of FOXC2 and MMP-9 in non-small cell lung cancer. Zhejiang Medical Journal. 2017;39:1564-6.
31. Zitvogel L, Kepp O, Galluzzi L, et al. Inflammasomes in carcinogenesis and anticancer immune responses. Nature Immunology. 2012;13:343-51.
32. Chen Y, Zheng W, Niu Z, et al. Caspase-1 affects the growth mediated by breast cancer and its regulation on myeloid inhibitory cell development. Chinese Journal of Immunology. 2013;29:1128-34.
33. Fernandes-Alnemri T, Wu J, Yu J W, et al. The pyroptosome: a supramolecular assembly of ASC dimers mediating inflammatory cell death via caspase-1 activation. Cell Death Differ. 2007;14:1590-604.
34. Kroemer G, Galluzzi L, Vandenabeele P, et al. Classification of cell death: recommendations of the Nomenclature Committee on Cell Death 2009. Cell Death Differ. 2009;16:3-11.

Figures

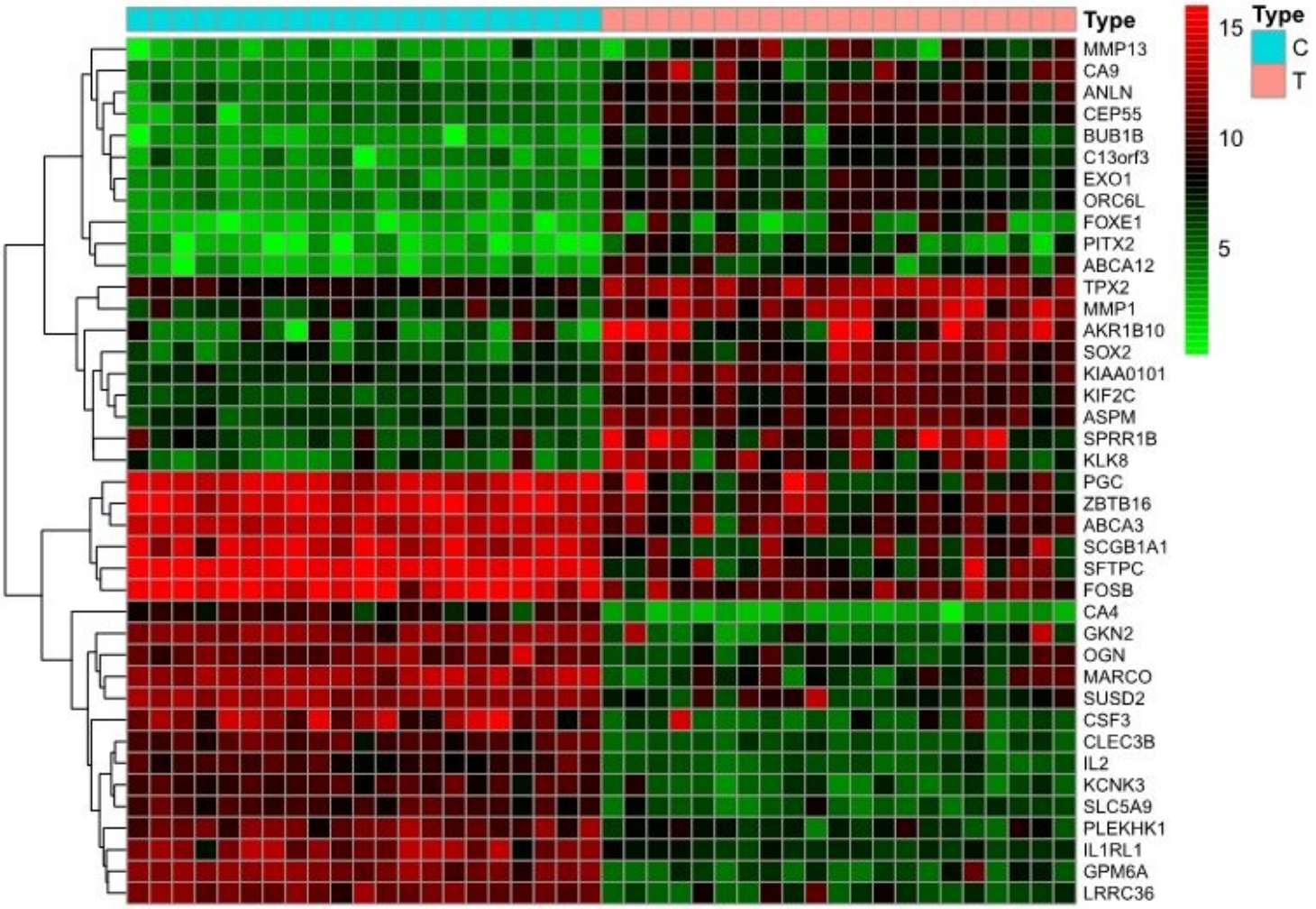

Figure 1

Heat map. The abscissa represents the clustering of samples, and the closer the gene expression between samples is, the closer it is. The ordinate represents gene clustering. The closer the gene expression is in the sample, the closer it is.

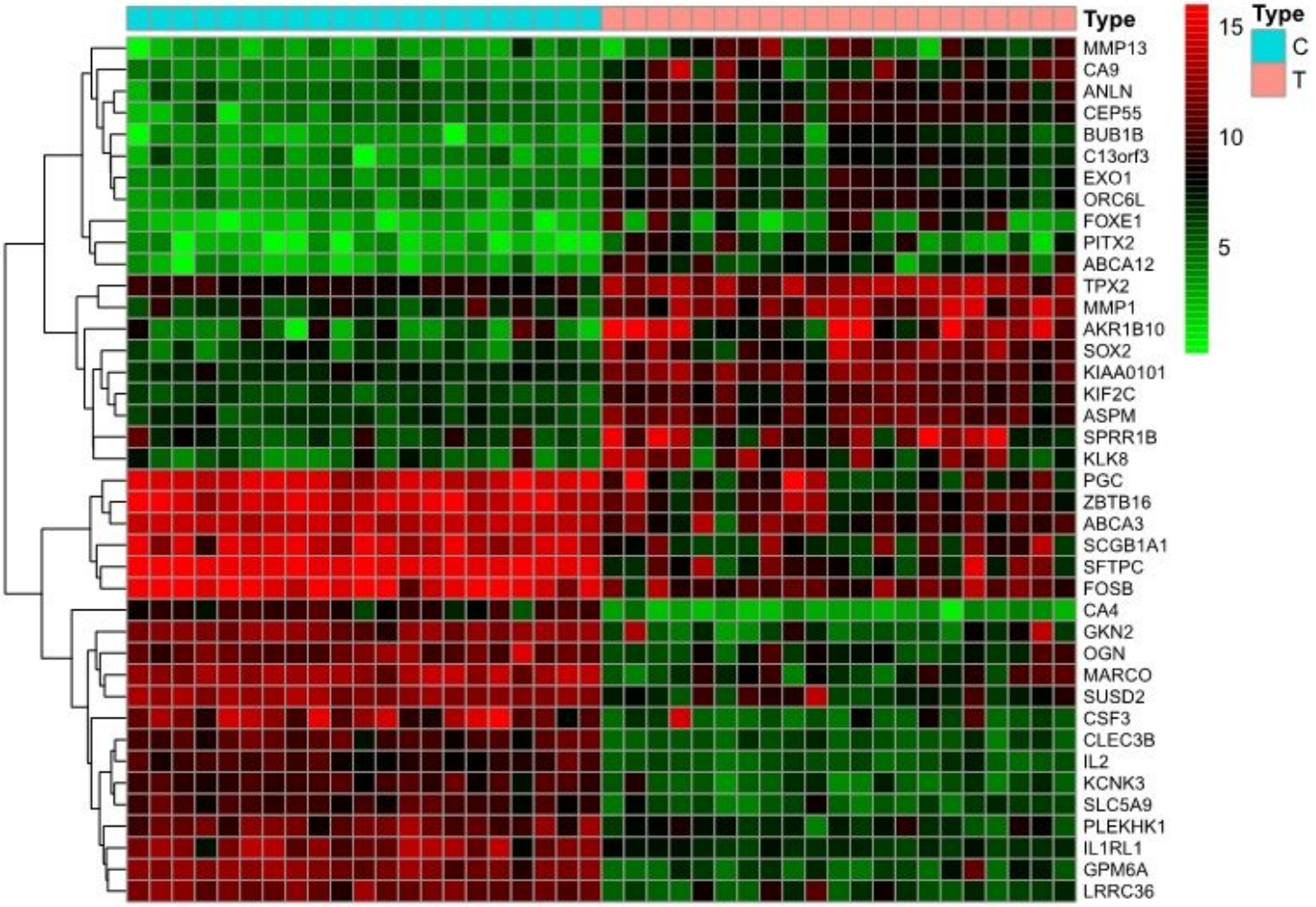

Figure 1

Heat map. The abscissa represents the clustering of samples, and the closer the gene expression between samples is, the closer it is. The ordinate represents gene clustering. The closer the gene expression is in the sample, the closer it is.

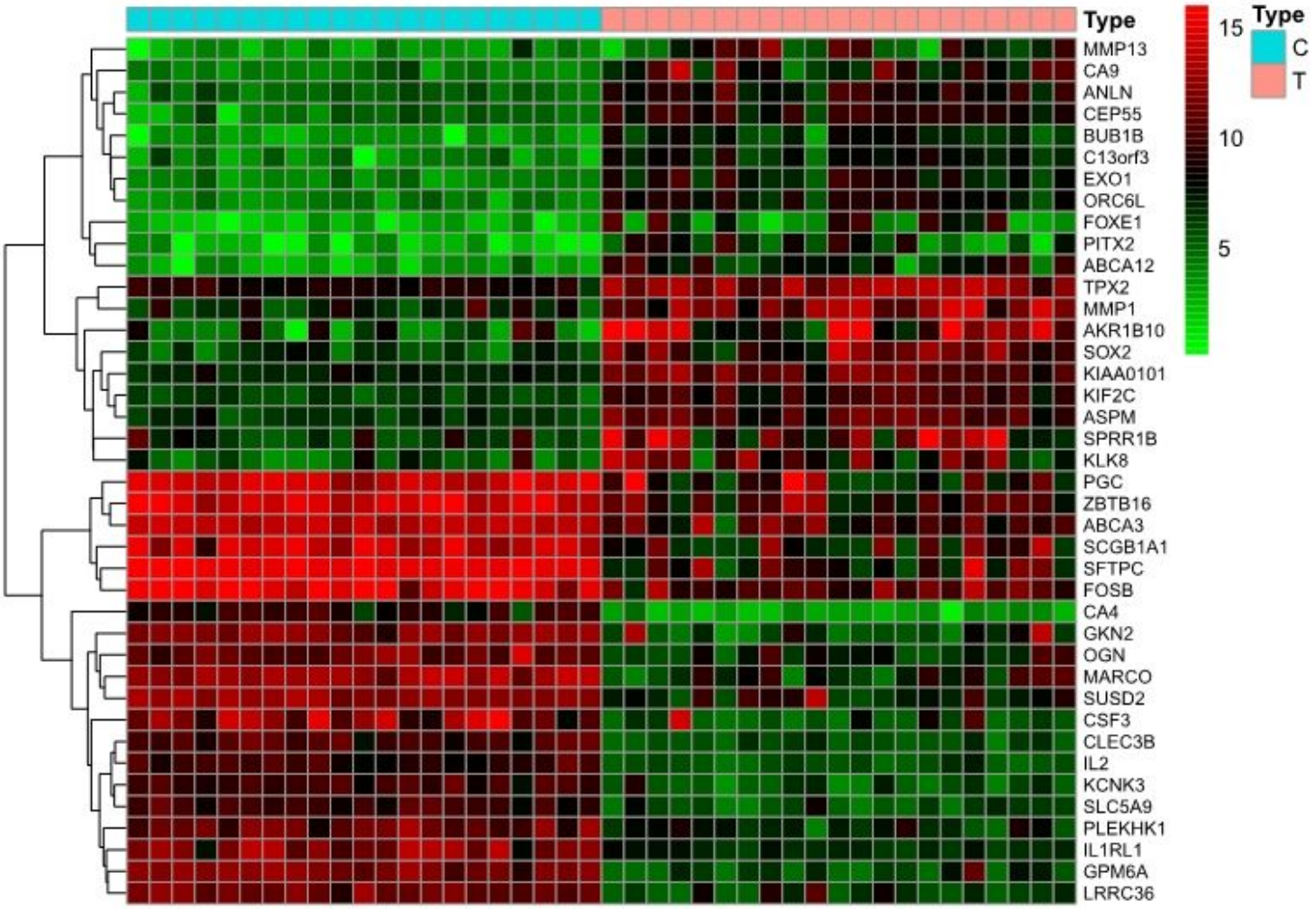

Figure 1

Heat map. The abscissa represents the clustering of samples, and the closer the gene expression between samples is, the closer it is. The ordinate represents gene clustering. The closer the gene expression is in the sample, the closer it is.

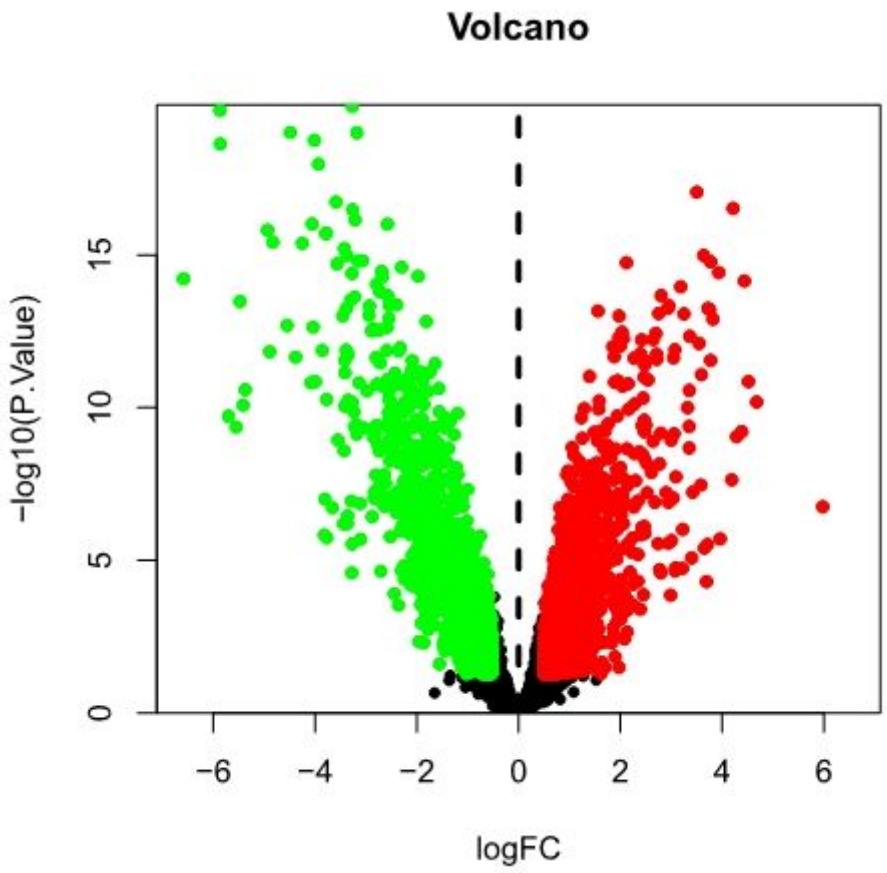

Figure 2

Volcano map. Each dot represents a gene, and the color is used to distinguish whether the gene is differentially expressed or not. The red dots represent up-regulated differentially expressed genes, the blue dots represent down-regulated differentially expressed genes, and the black dots represent genes that are not differentially expressed.

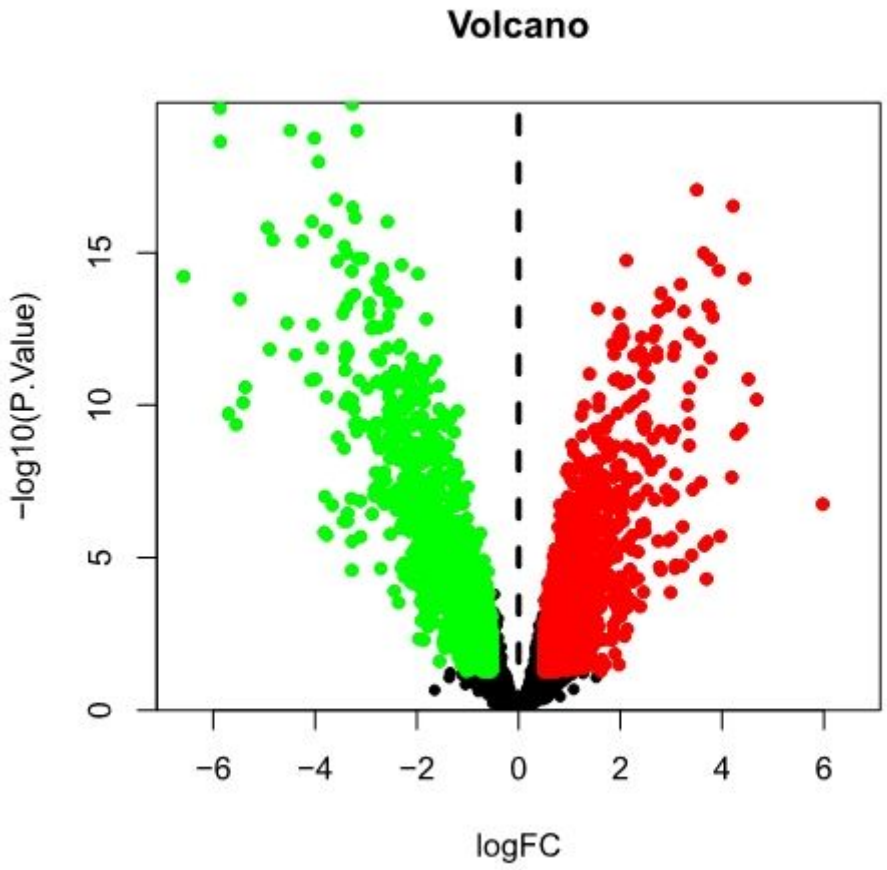

Figure 2

Volcano map. Each dot represents a gene, and the color is used to distinguish whether the gene is differentially expressed or not. The red dots represent up-regulated differentially expressed genes, the blue dots represent down-regulated differentially expressed genes, and the black dots represent genes that are not differentially expressed.

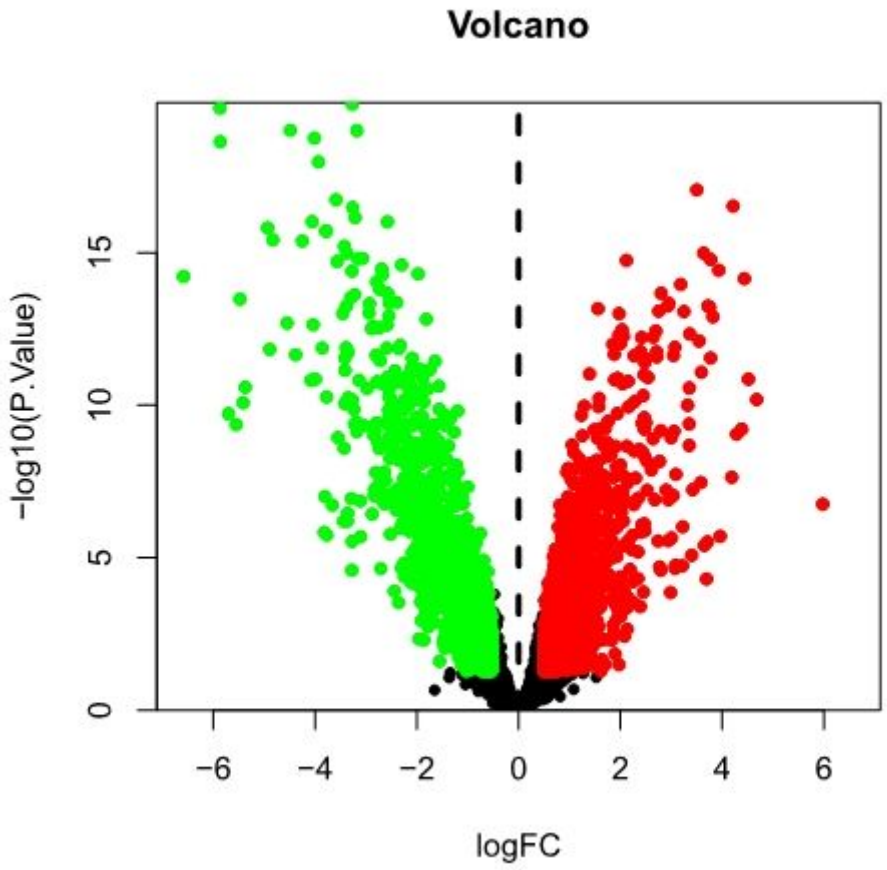

Figure 2

Volcano map. Each dot represents a gene, and the color is used to distinguish whether the gene is differentially expressed or not. The red dots represent up-regulated differentially expressed genes, the blue dots represent down-regulated differentially expressed genes, and the black dots represent genes that are not differentially expressed.

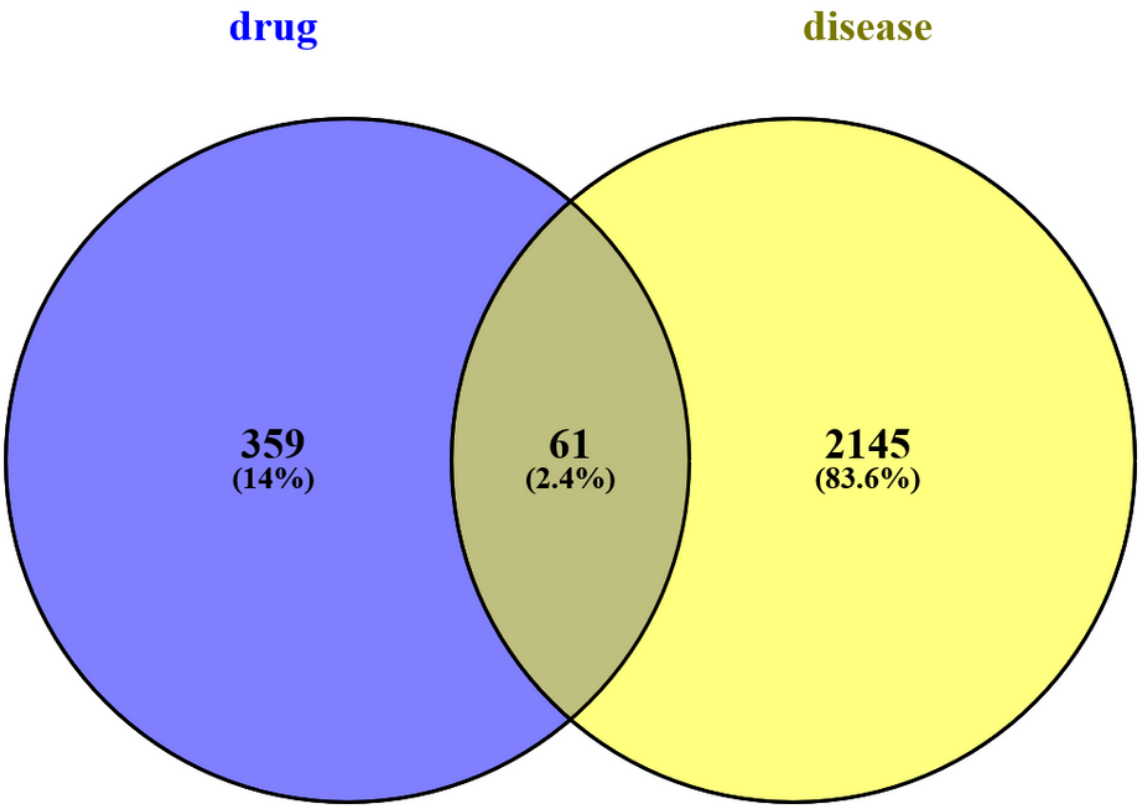

Figure 3

intersection targets

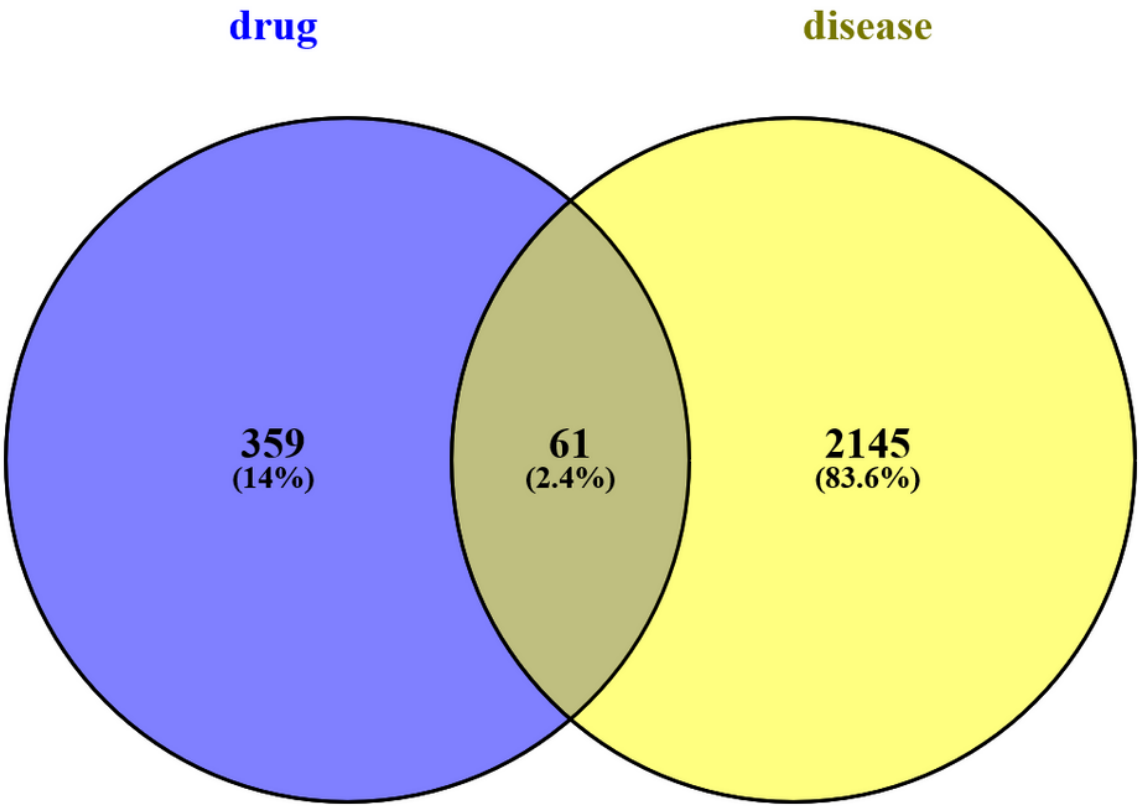

Figure 3

intersection targets

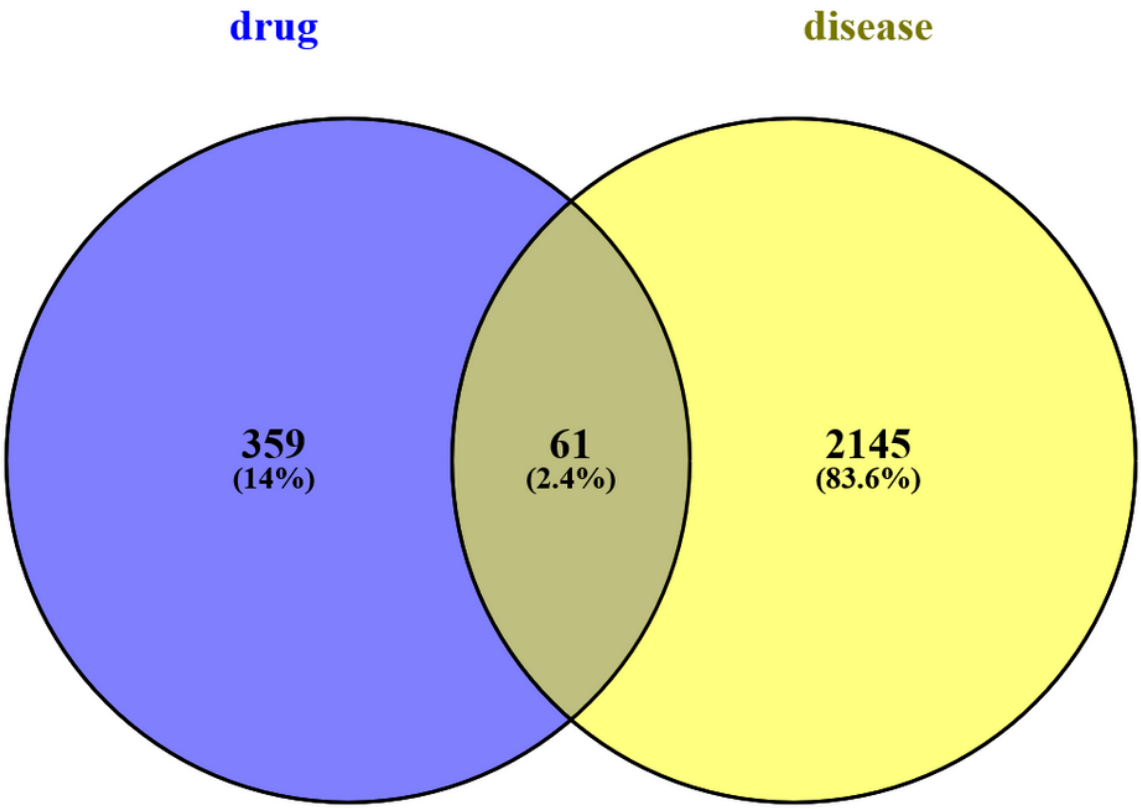

Figure 3

intersection targets

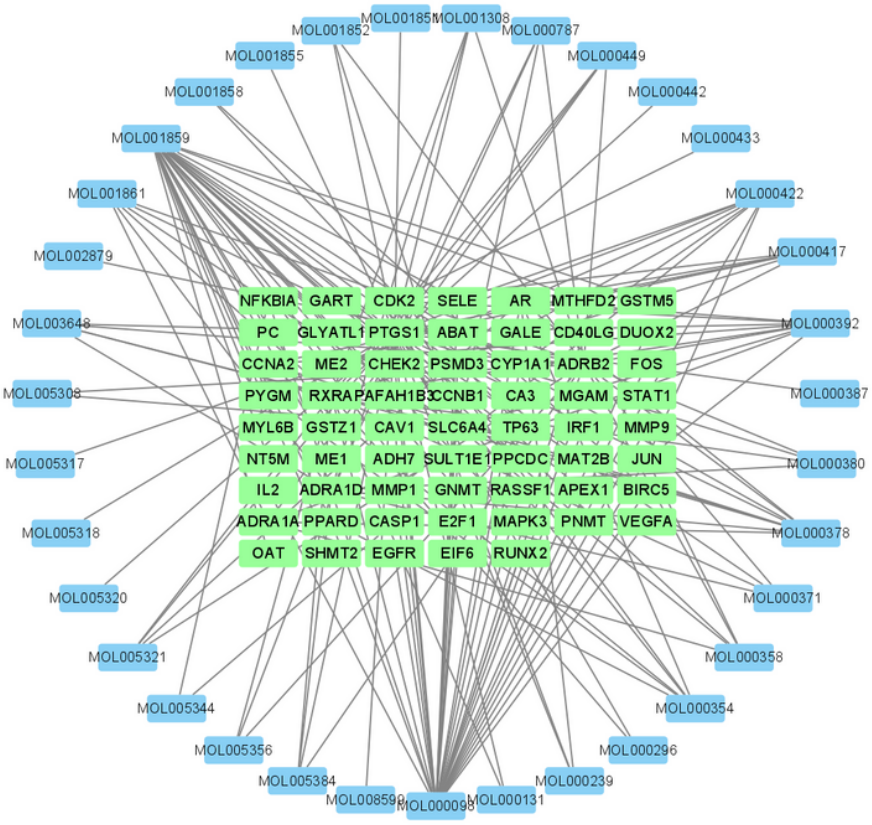

Figure 4

Disease-Compound-Target Network

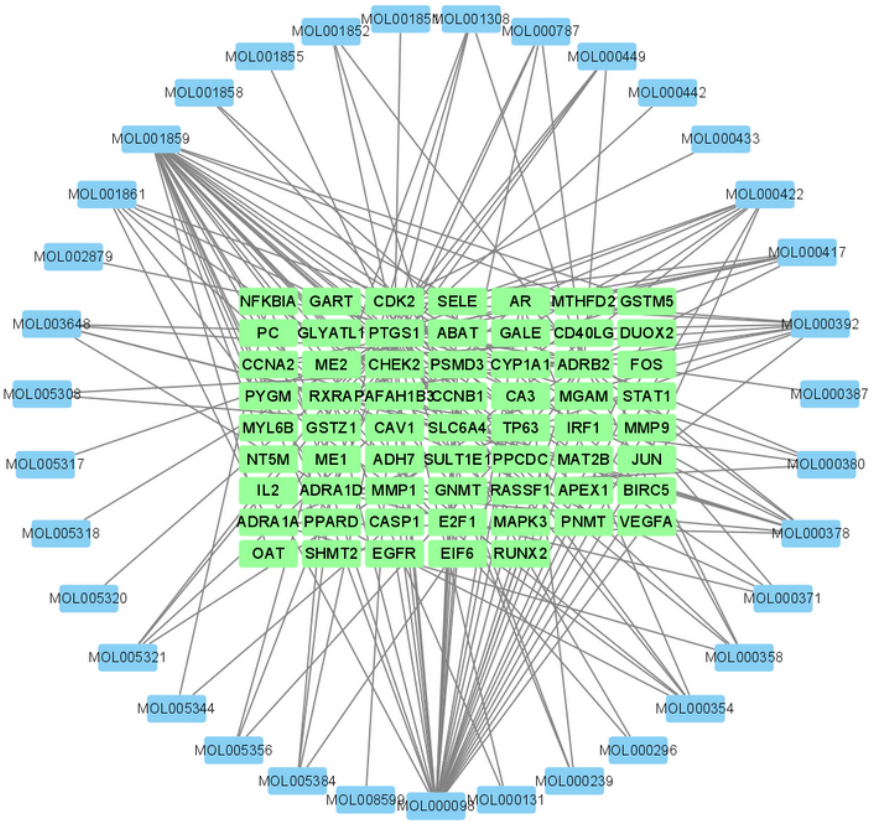

Figure 4

Disease-Compound-Target Network

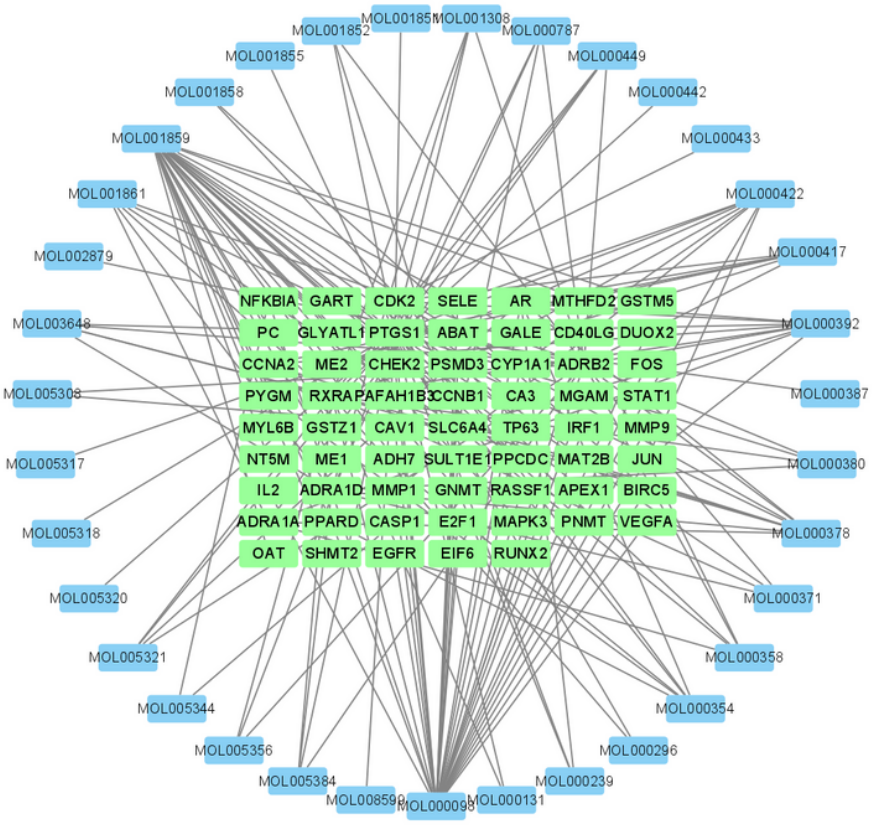

Figure 4

Disease-Compound-Target Network

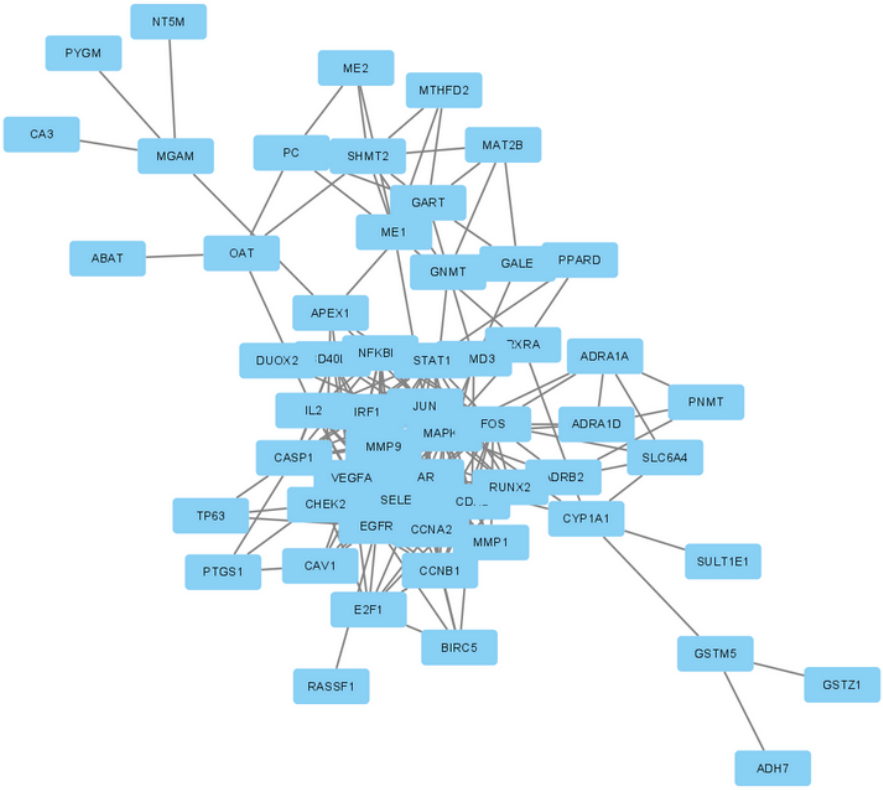

Figure 5

PPI network

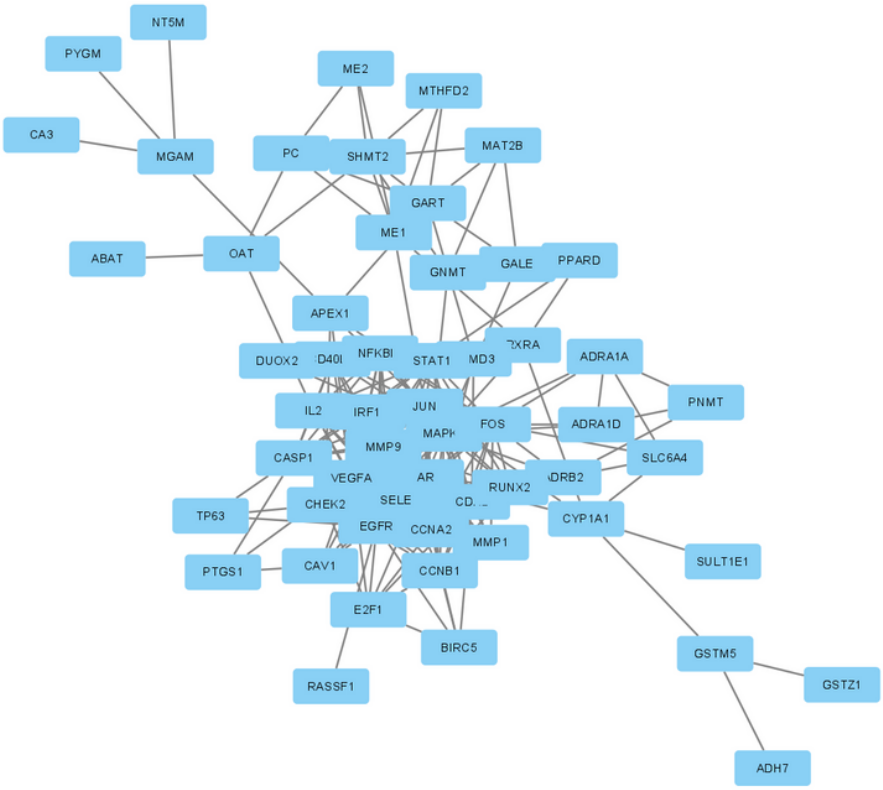

Figure 5

PPI network

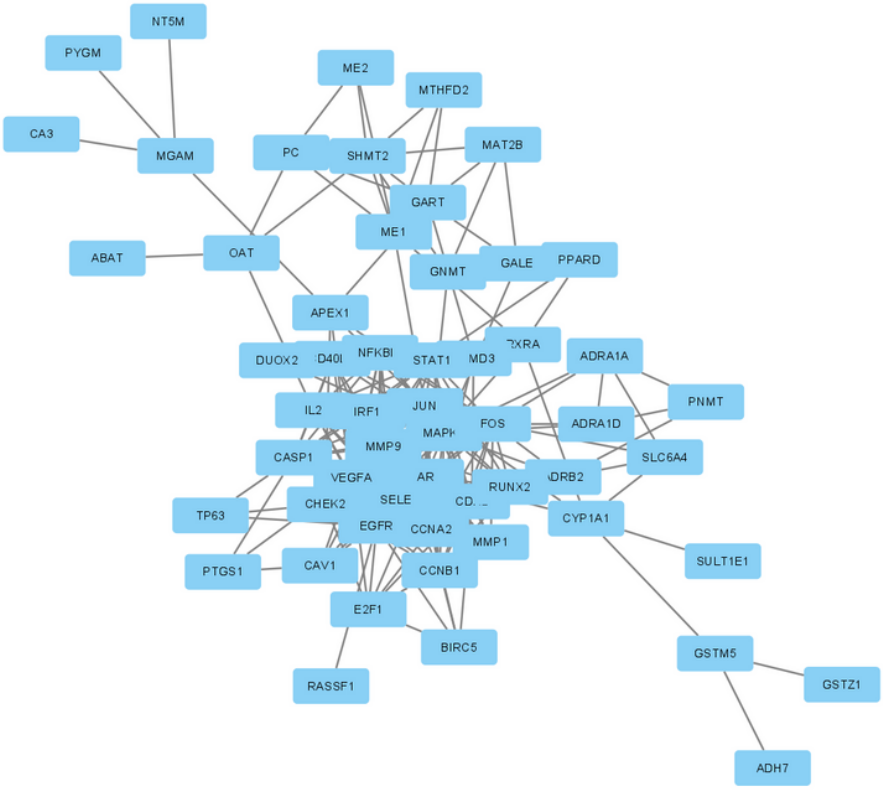

Figure 5

PPI network

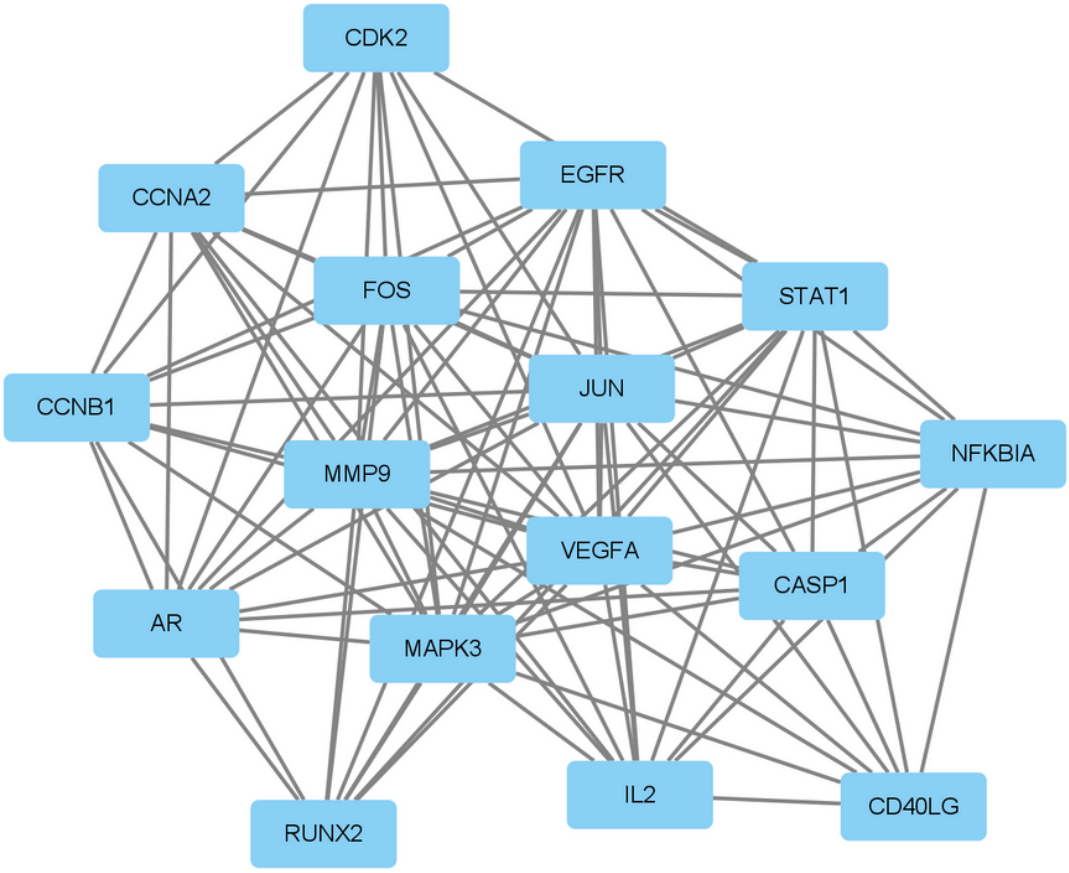

Figure 6

PPI network (select the targets which Degree value (≥7))

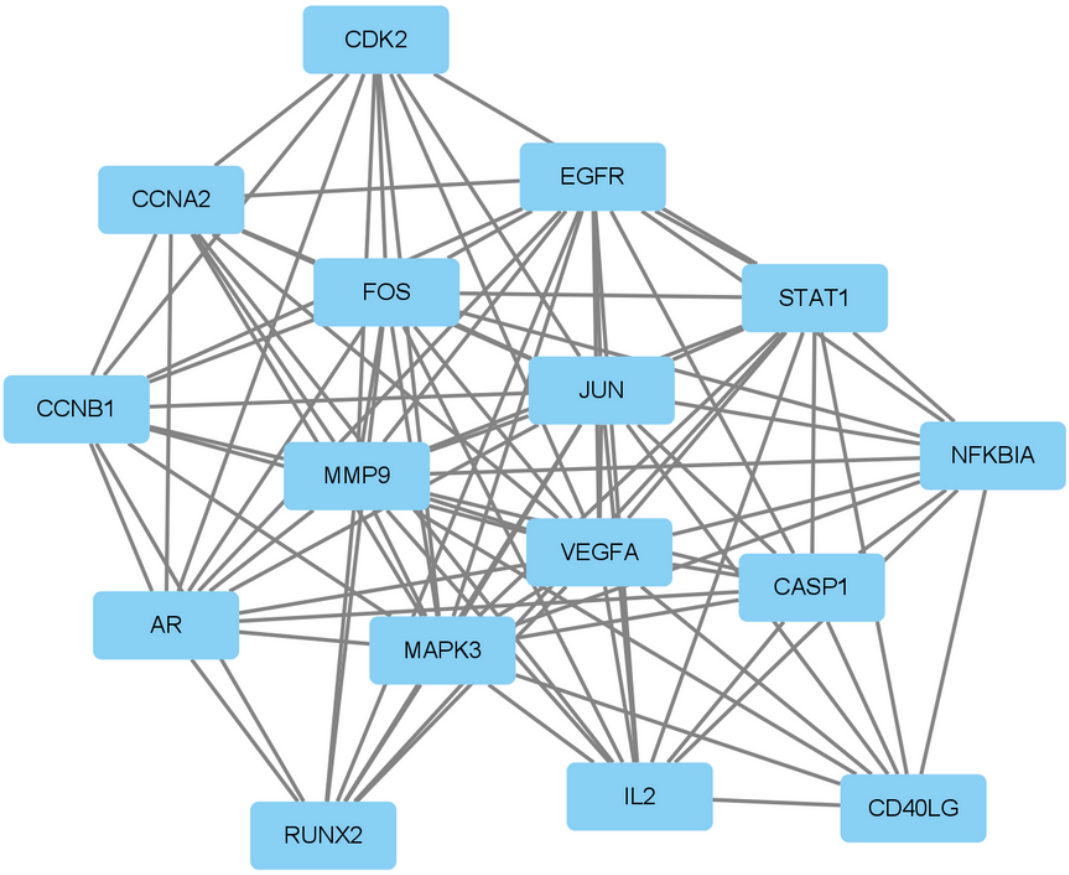

Figure 6

PPI network (select the targets which Degree value (≥7))

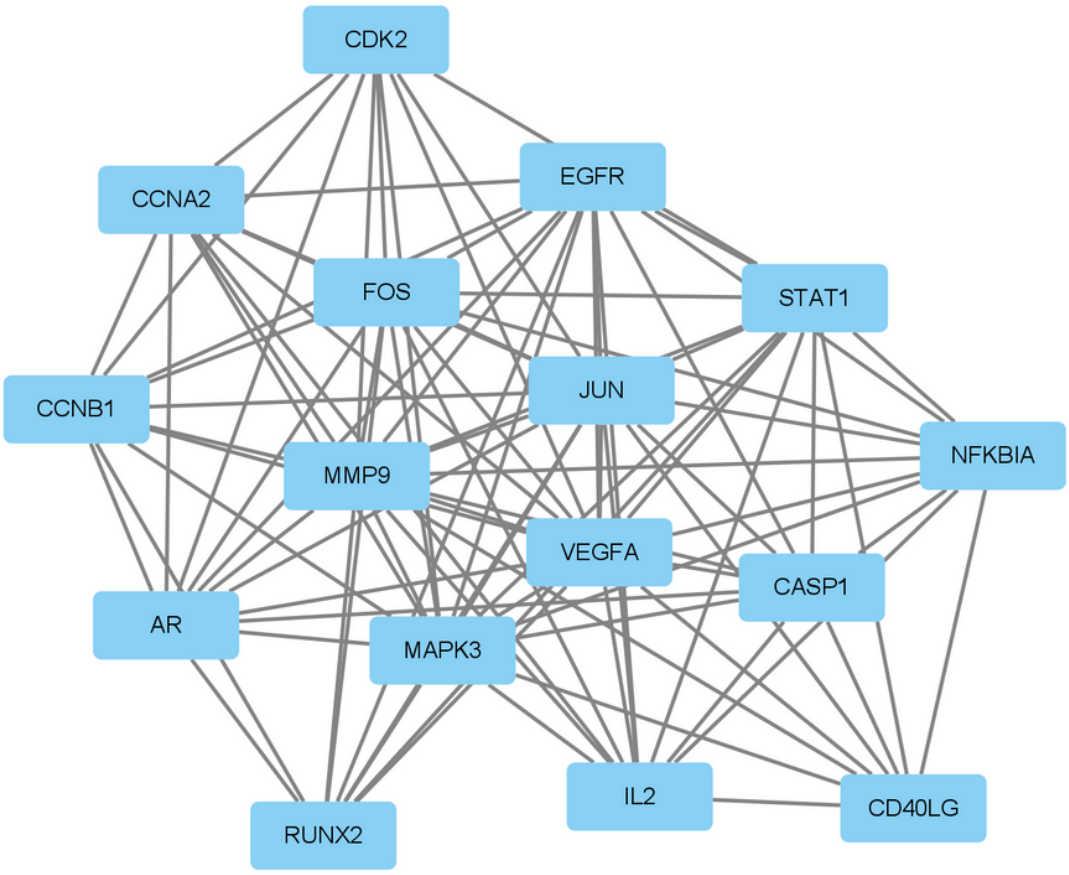

Figure 6

PPI network (select the targets which Degree value (≥7))

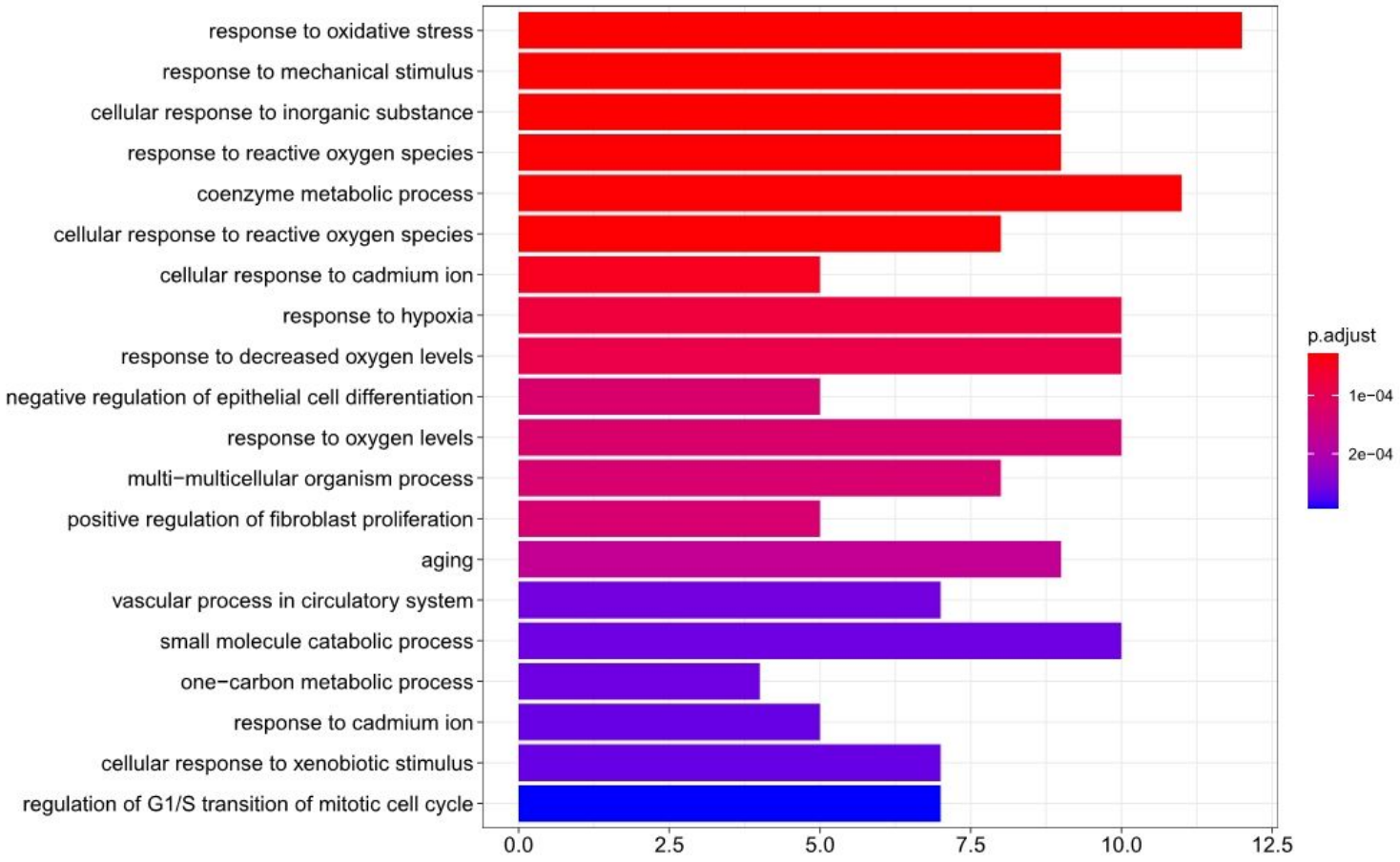

Figure 7

GO Enrichment—BP. Top 20 biology process from GO enrichment

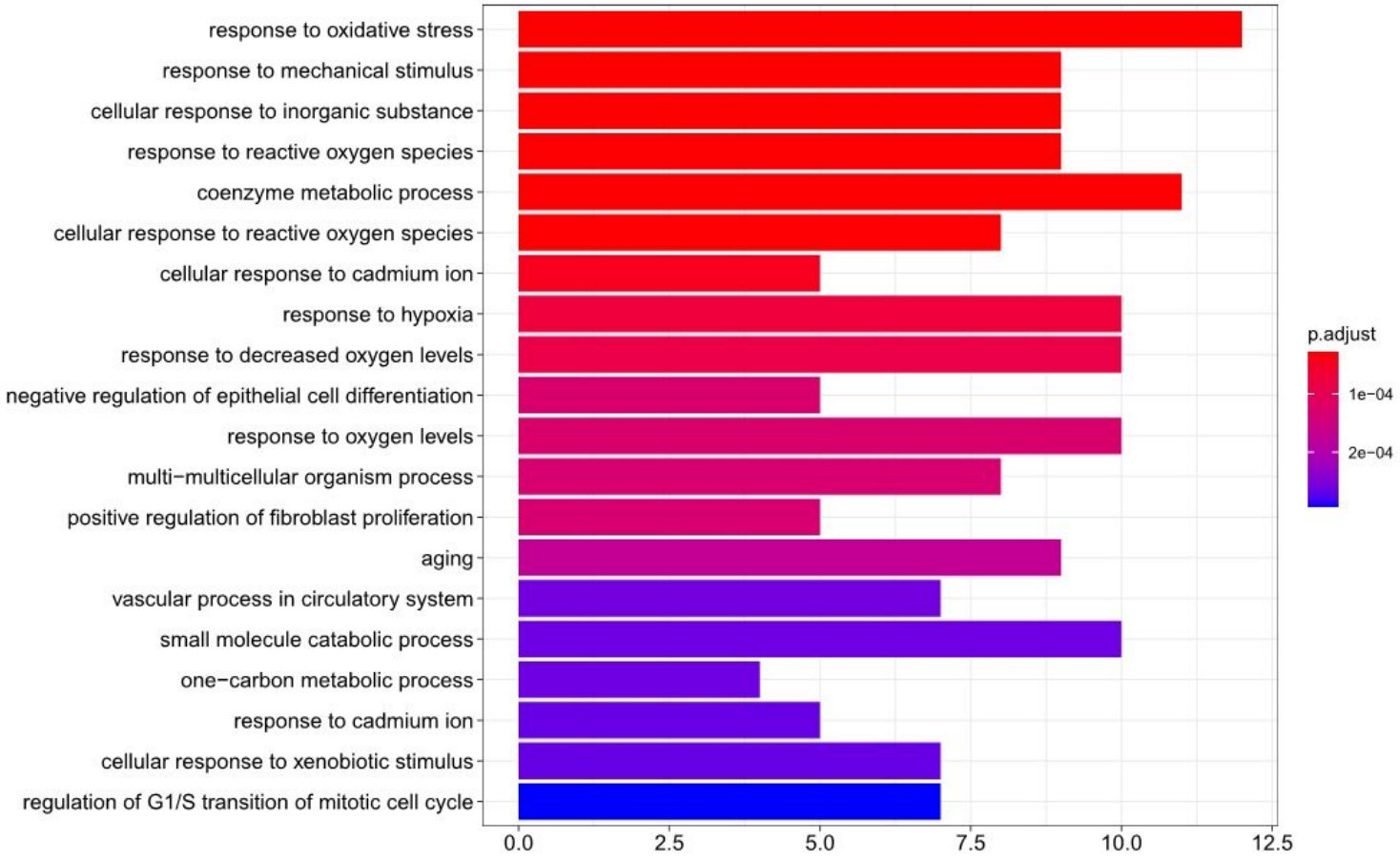

Figure 7

GO Enrichment—BP. Top 20 biology process from GO enrichment

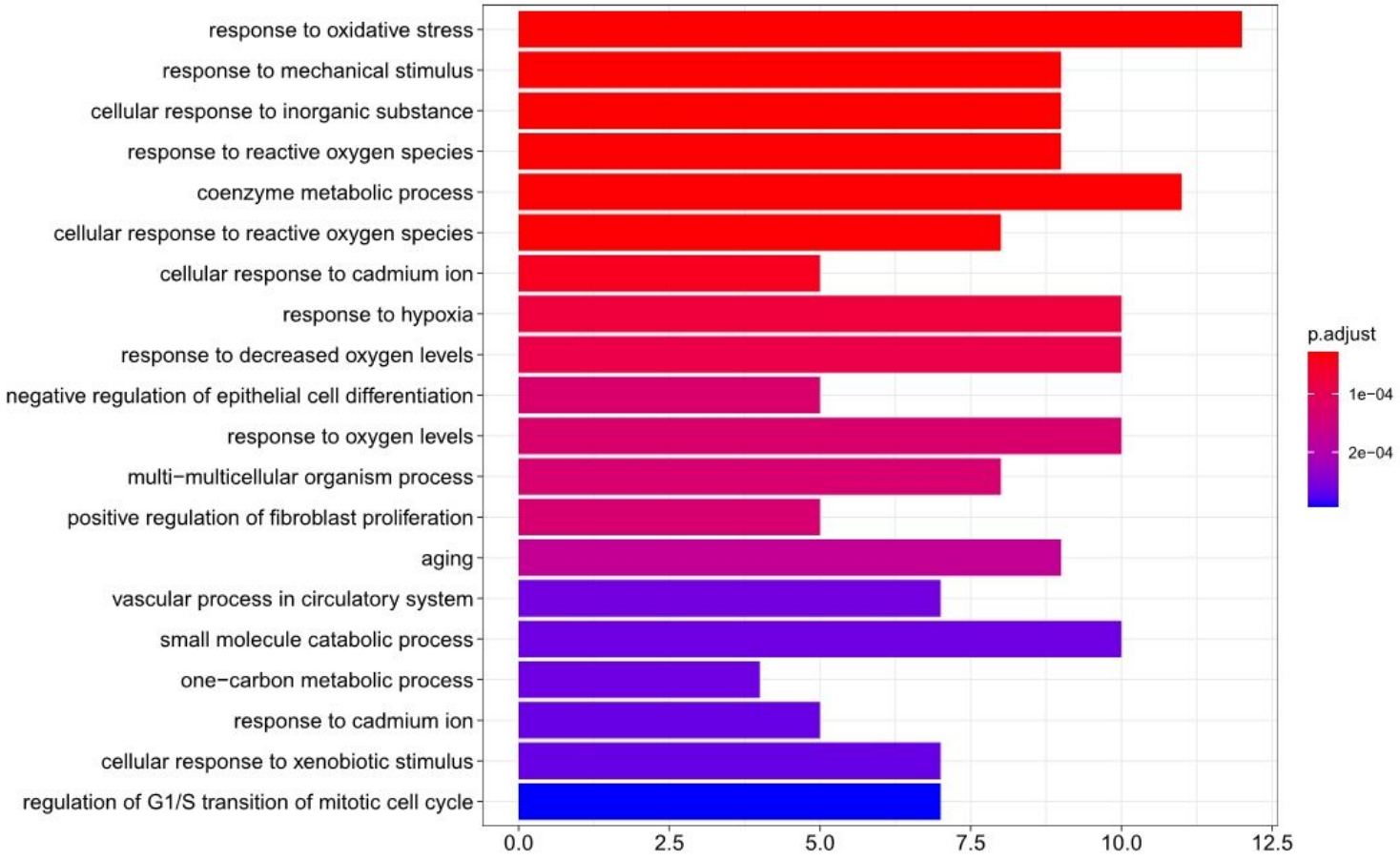

Figure 7

GO Enrichment—BP. Top 20 biology process from GO enrichment

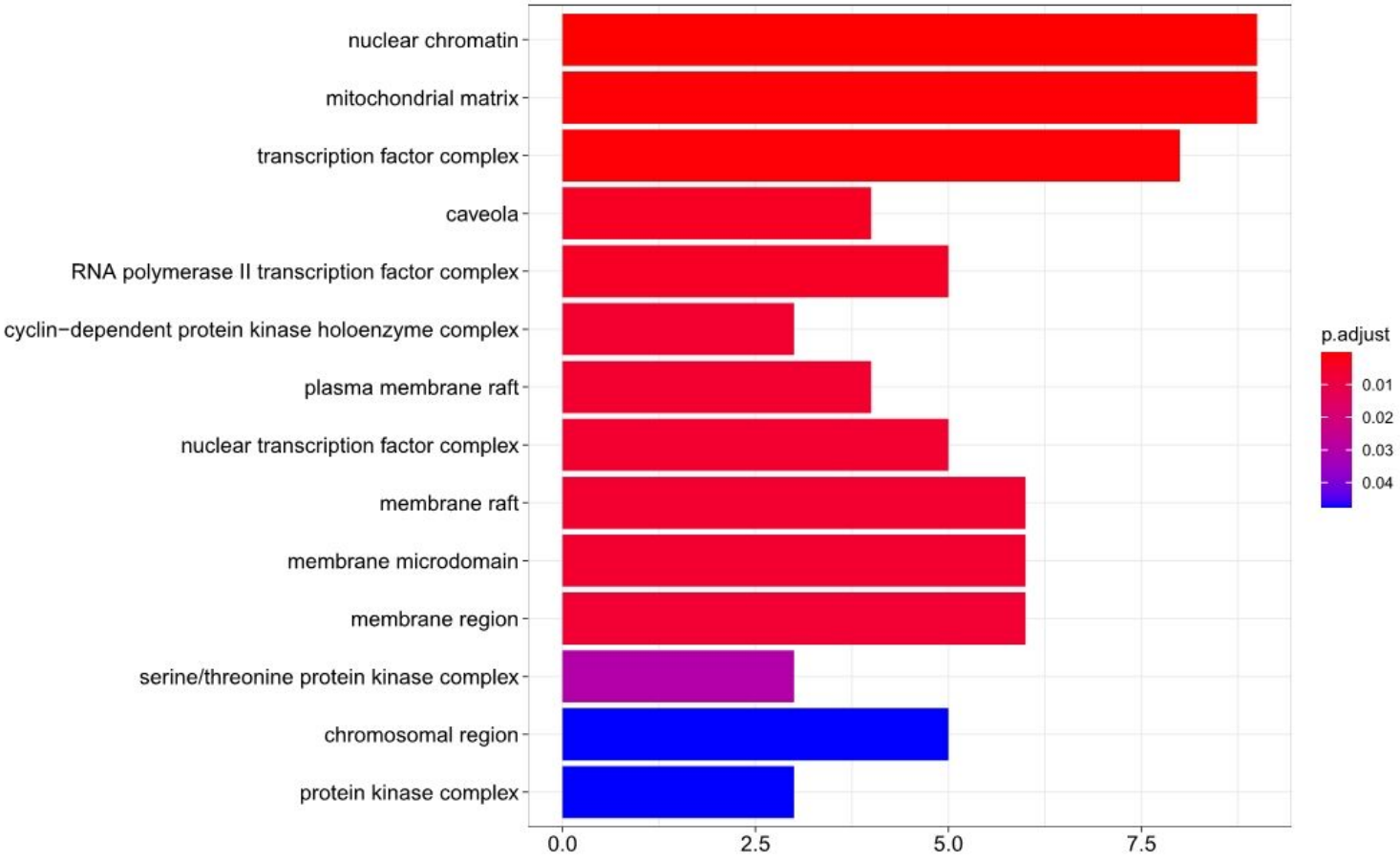

Figure 8

GO enrichment—CC. Top 20 molecular function from GO enrichment

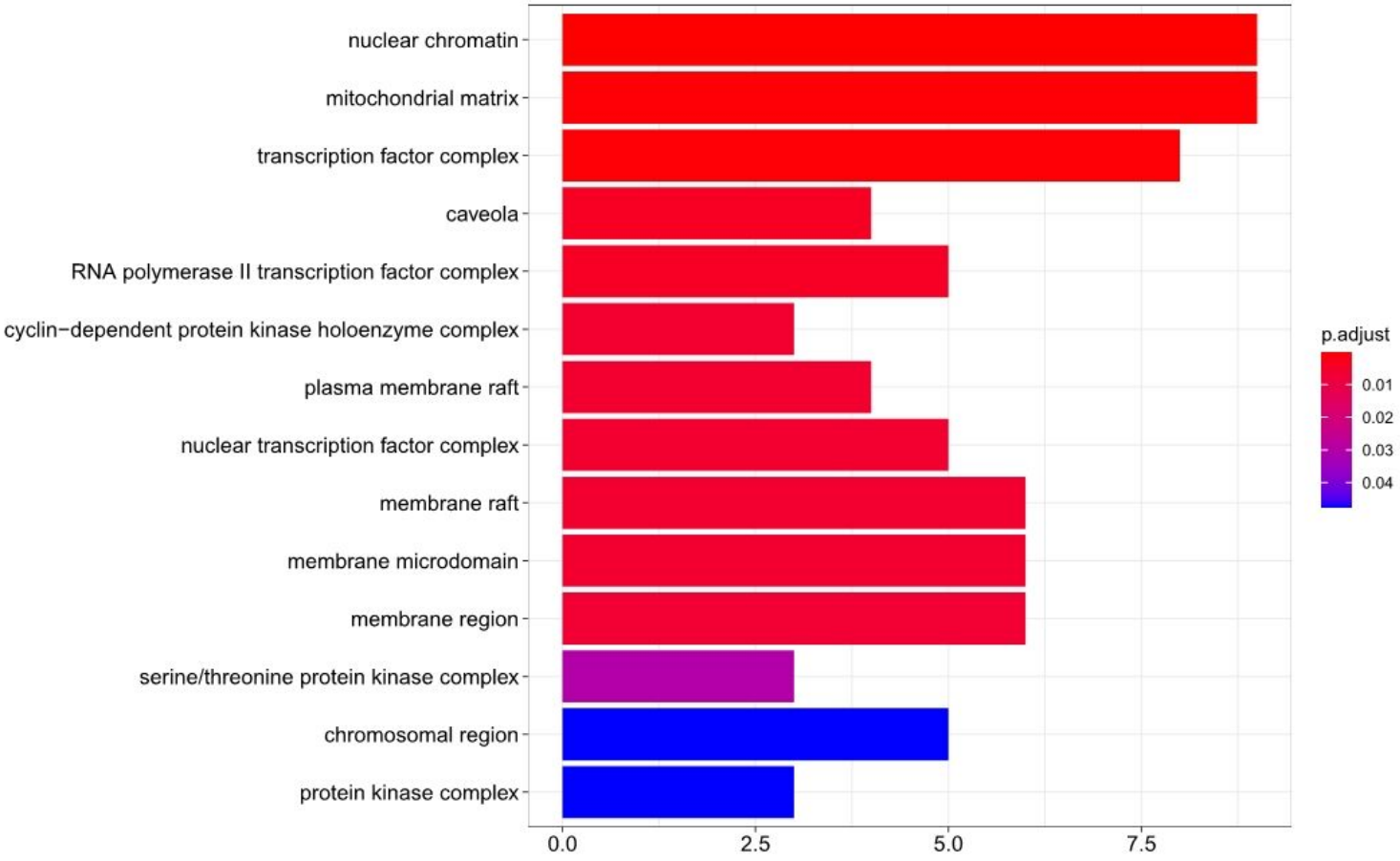

Figure 8

GO enrichment—CC. Top 20 molecular function from GO enrichment

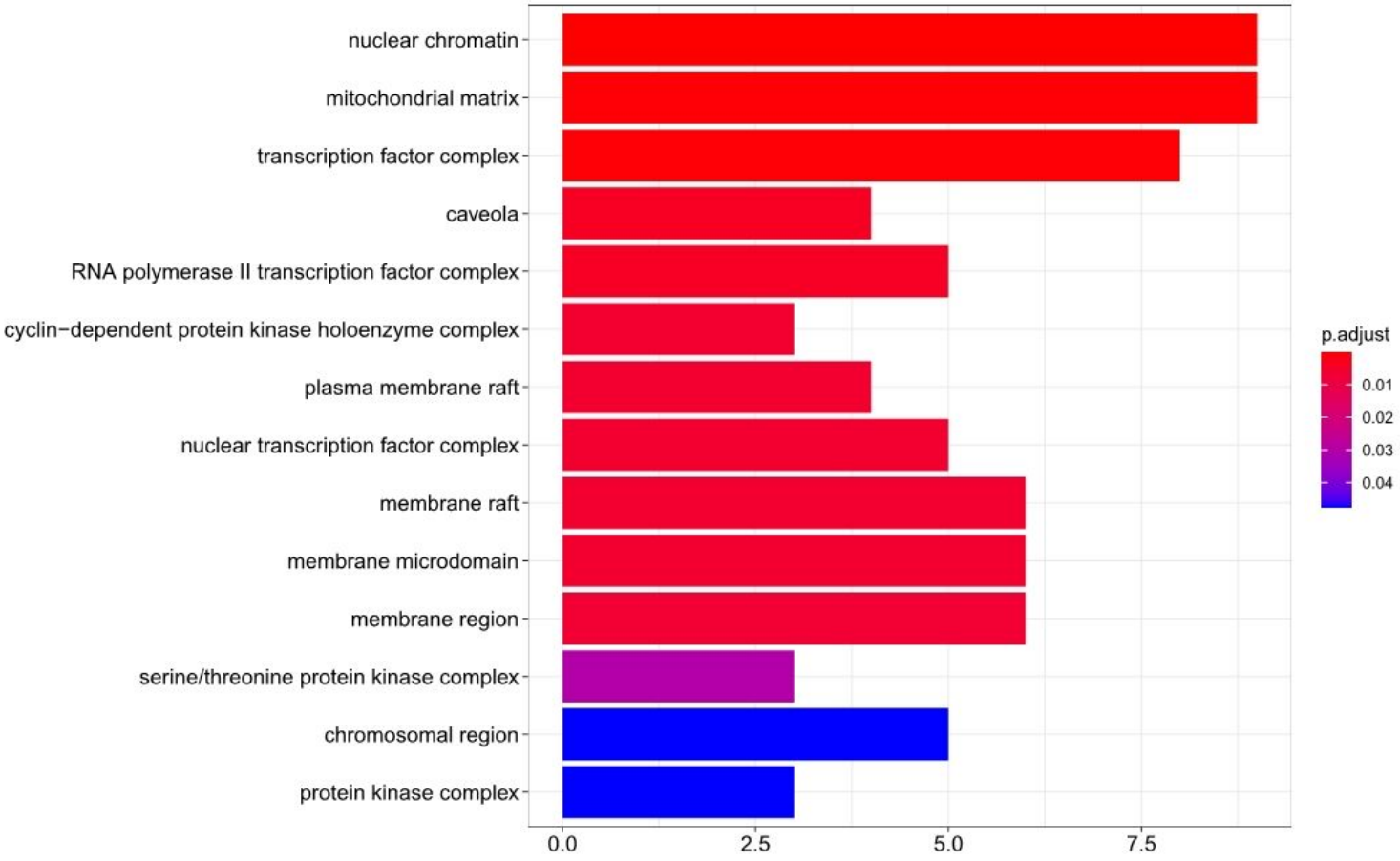

Figure 8

GO enrichment—CC. Top 20 molecular function from GO enrichment

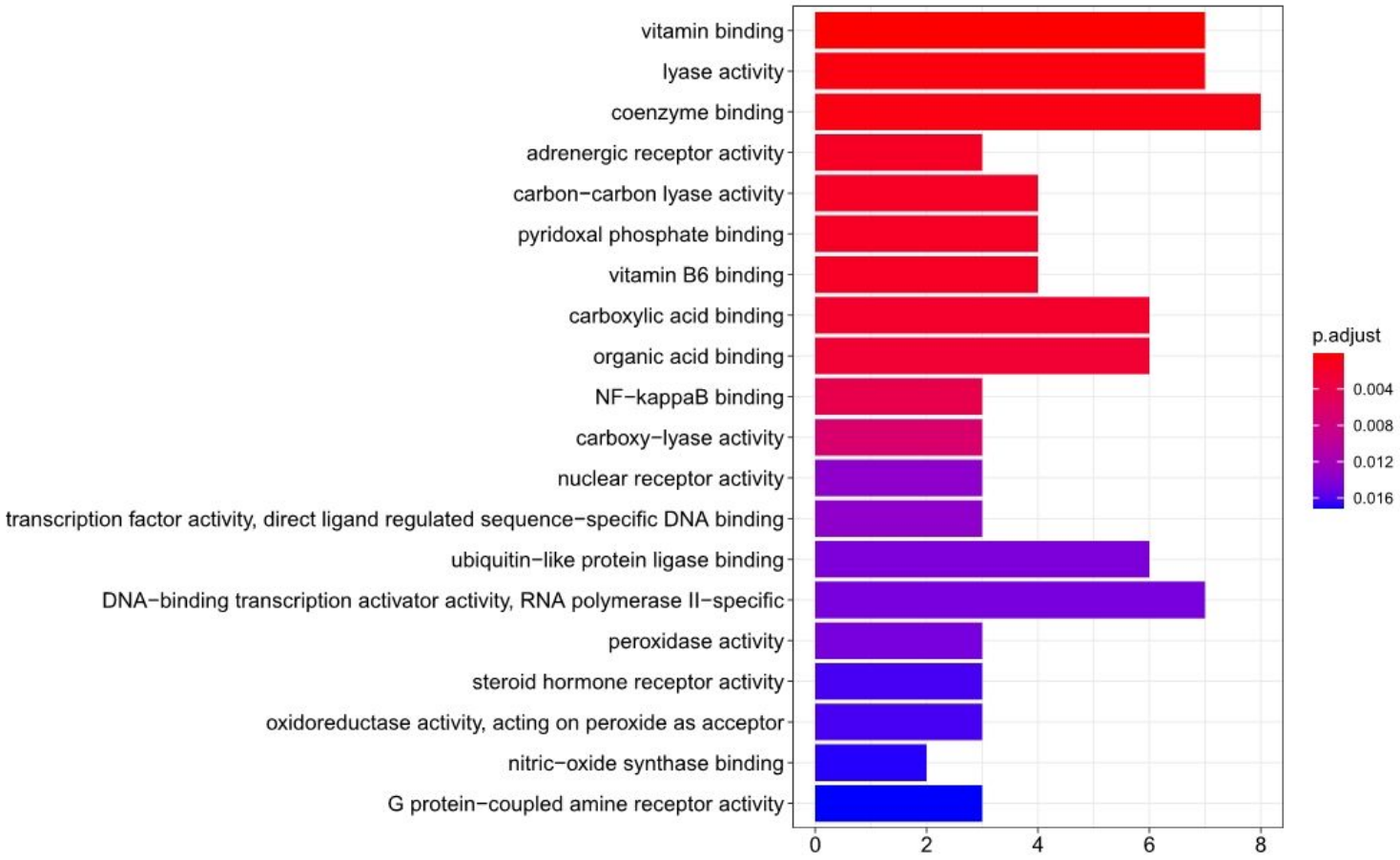

Figure 9

GO enrichment—MF. cellular component from GO enrichment

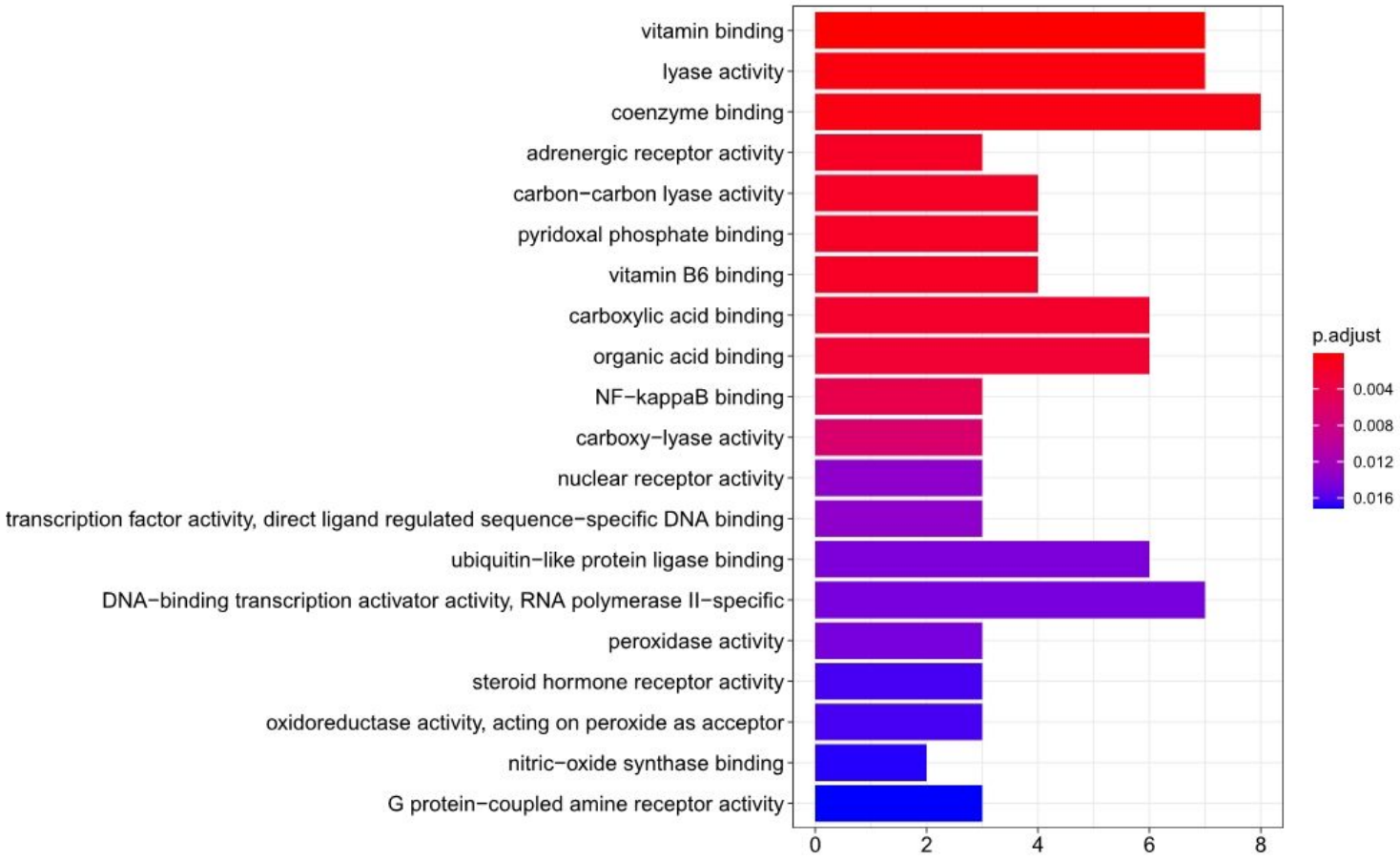

Figure 9

GO enrichment—MF. cellular component from GO enrichment

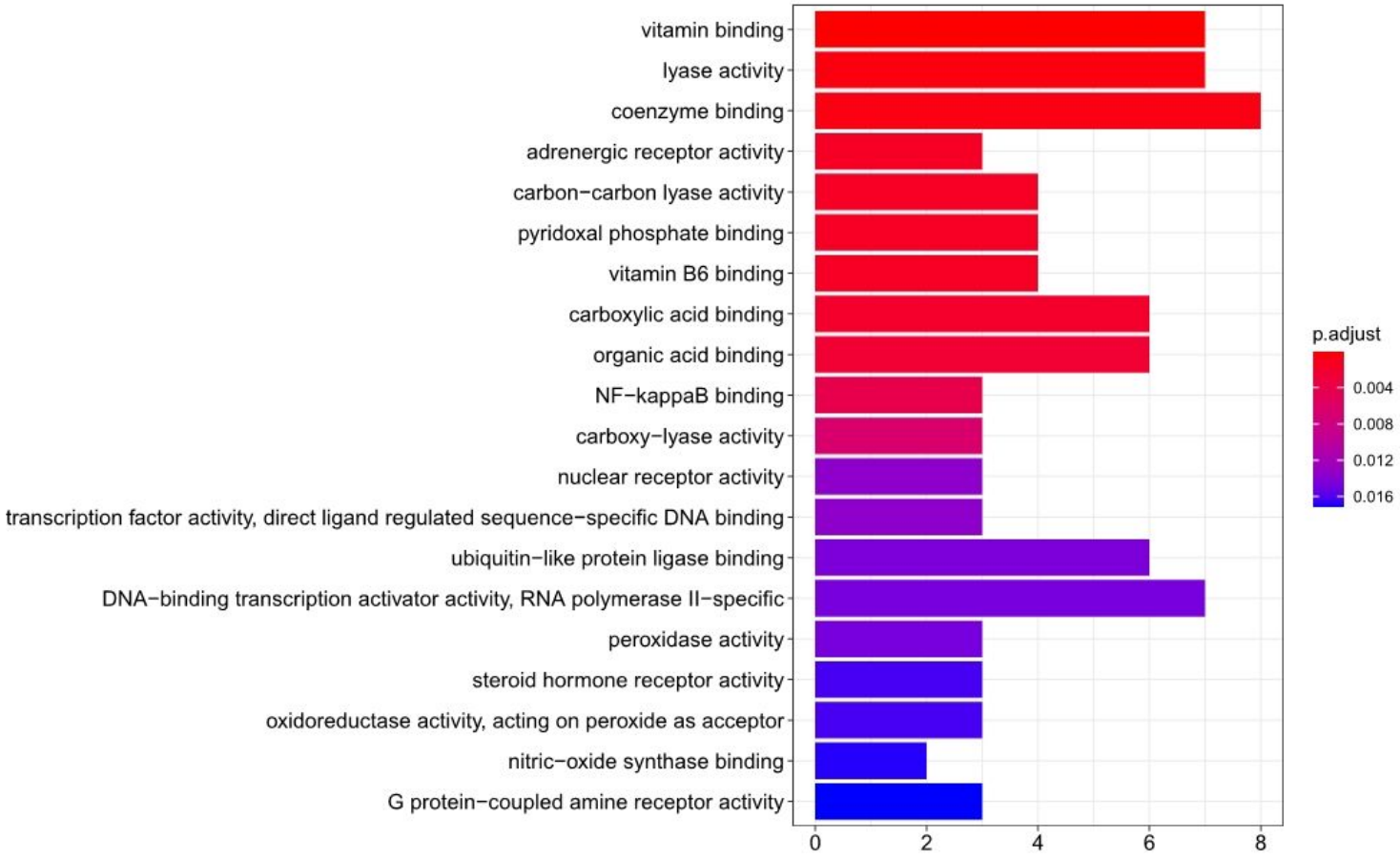

Figure 9

GO enrichment—MF. cellular component from GO enrichment

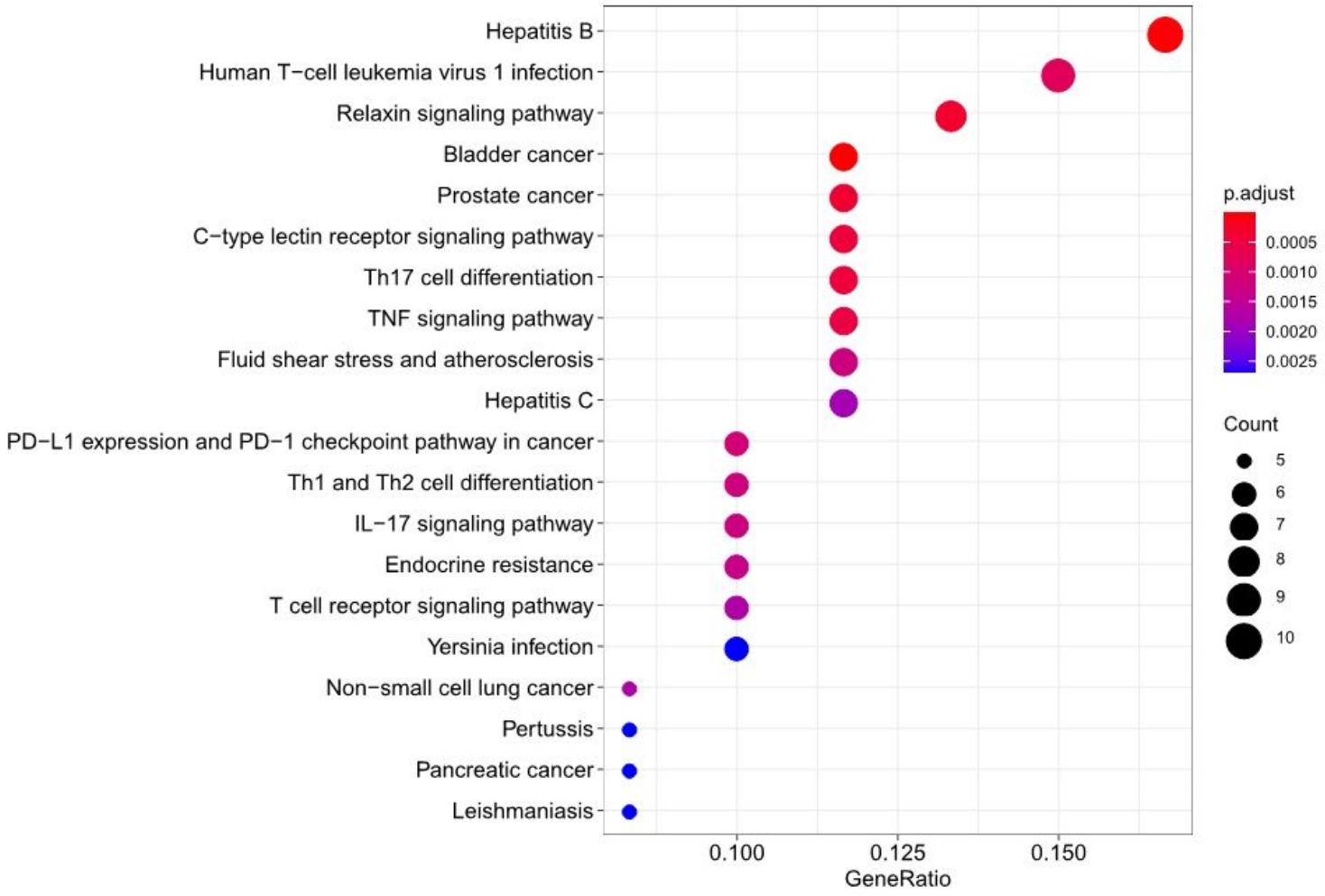

Figure 10

Pathway analysis. Dot plot of the top10 KEGG pathway

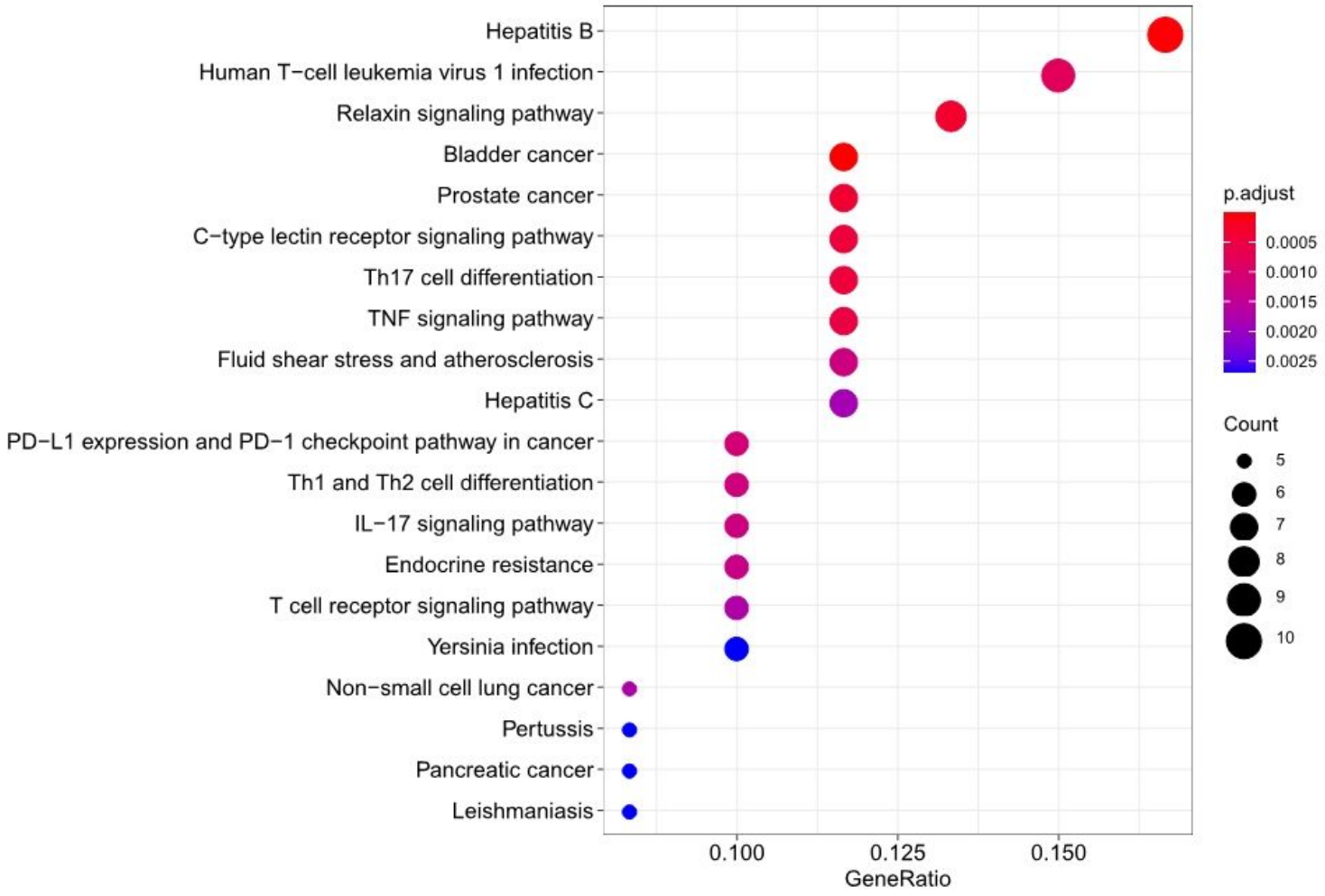

Figure 10

Pathway analysis. Dot plot of the top10 KEGG pathway

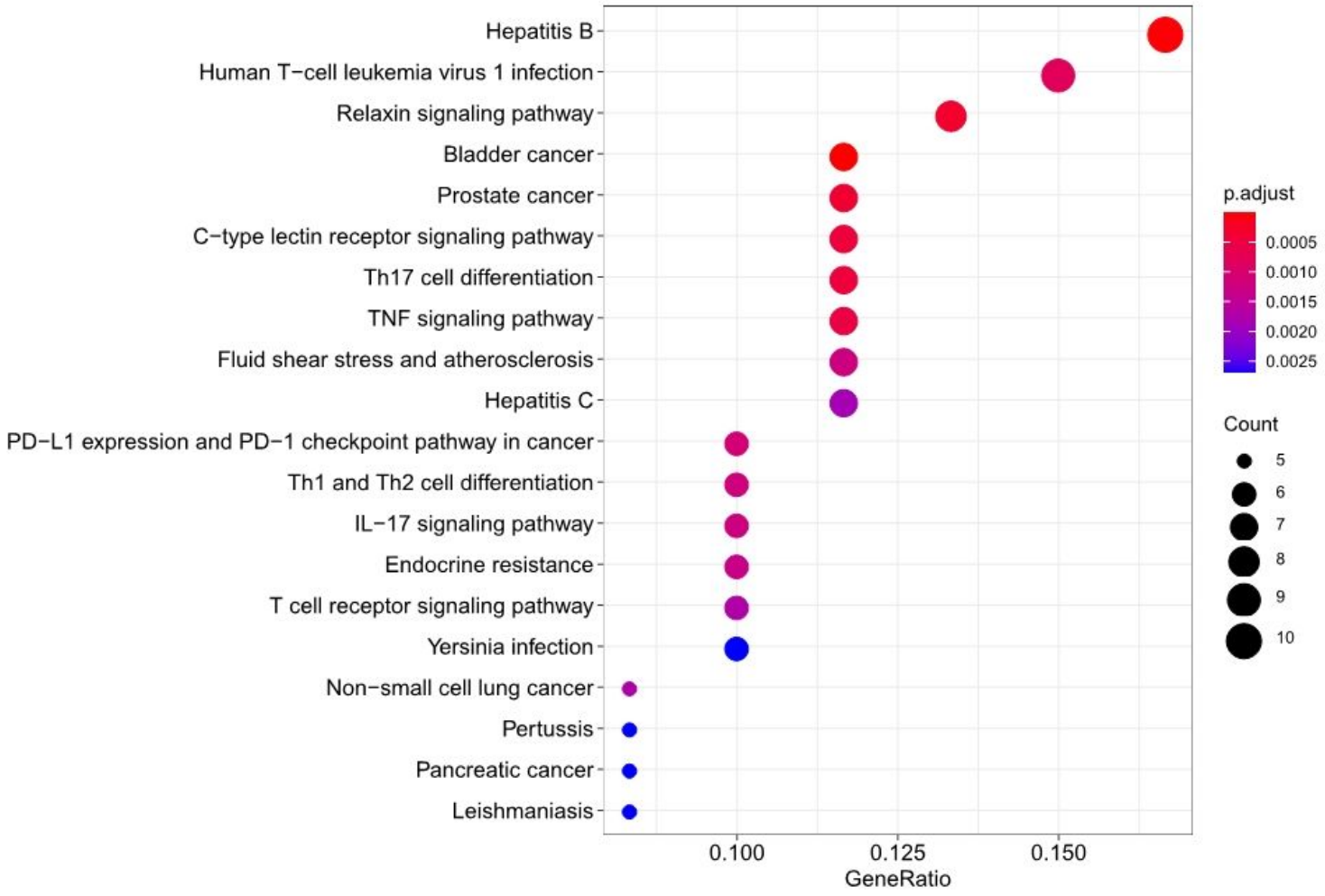

Figure 10

Pathway analysis. Dot plot of the top10 KEGG pathway

Supplementary Files

This is a list of supplementary files associated with this preprint. Click to download.

- Additionalfile1.doc
- Additionalfile1.doc
- Additionalfile1.doc